Interactions of electron with atoms and molecules
Rotational and vibrational excitation

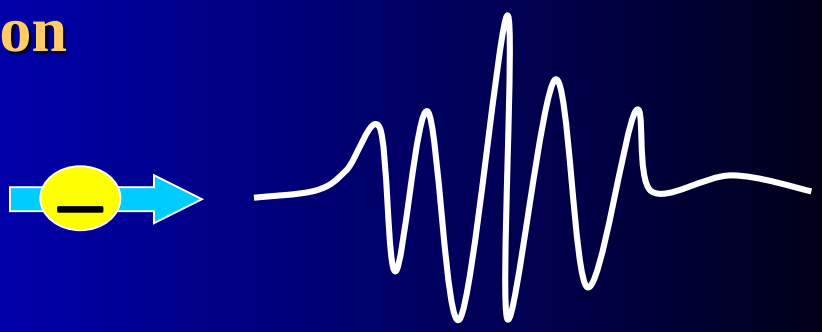

Rutherford atom

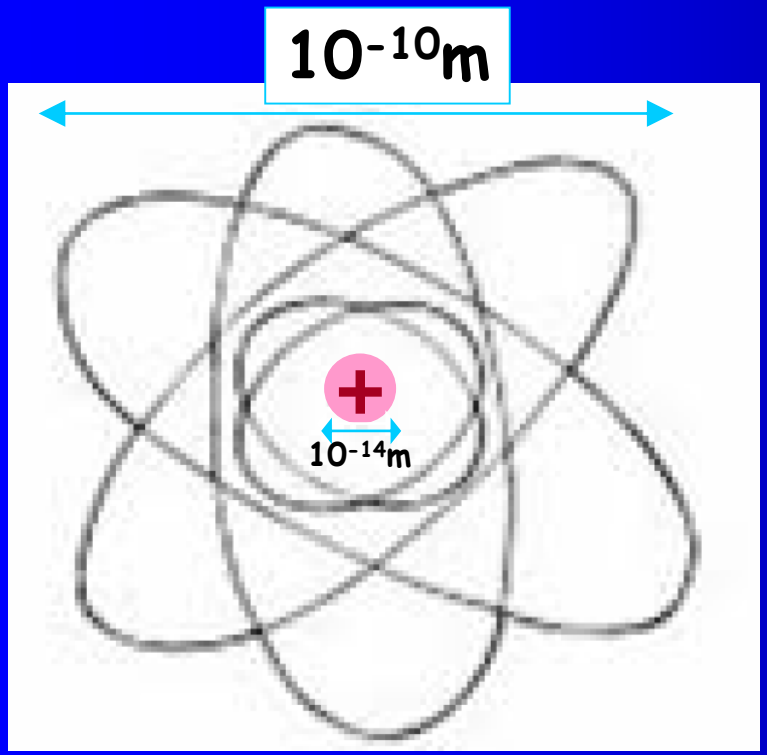

molecule H_2^+

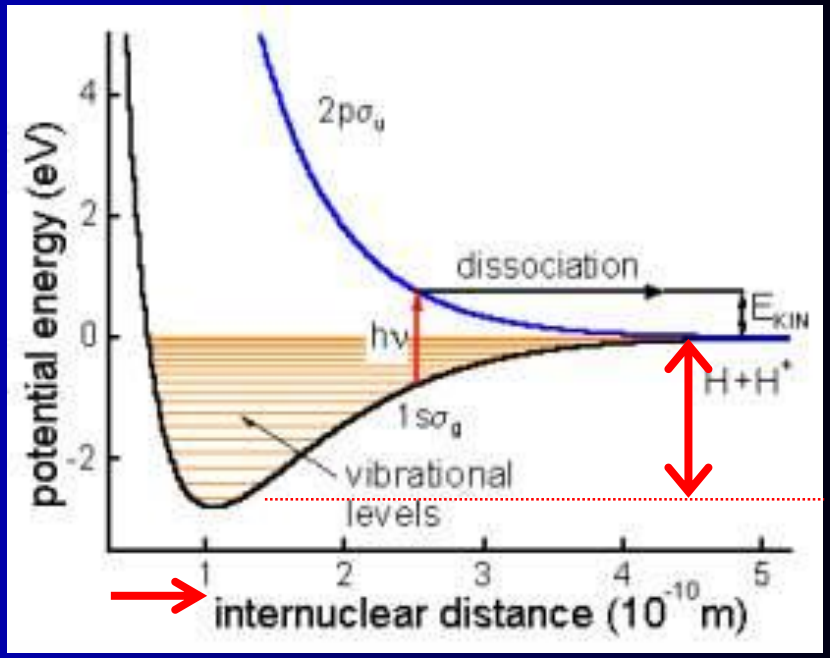

Single collision

$$H_2^+ + Ar \Rightarrow ArH^+ + H$$

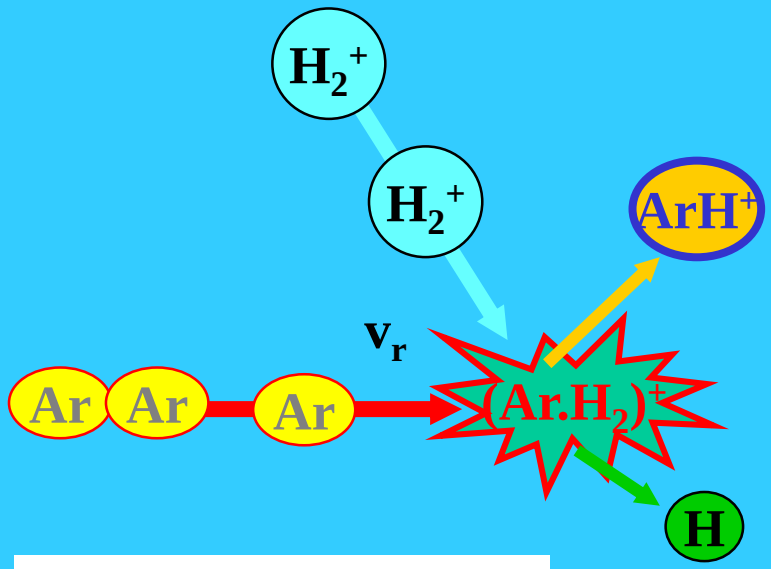

reaction cross section

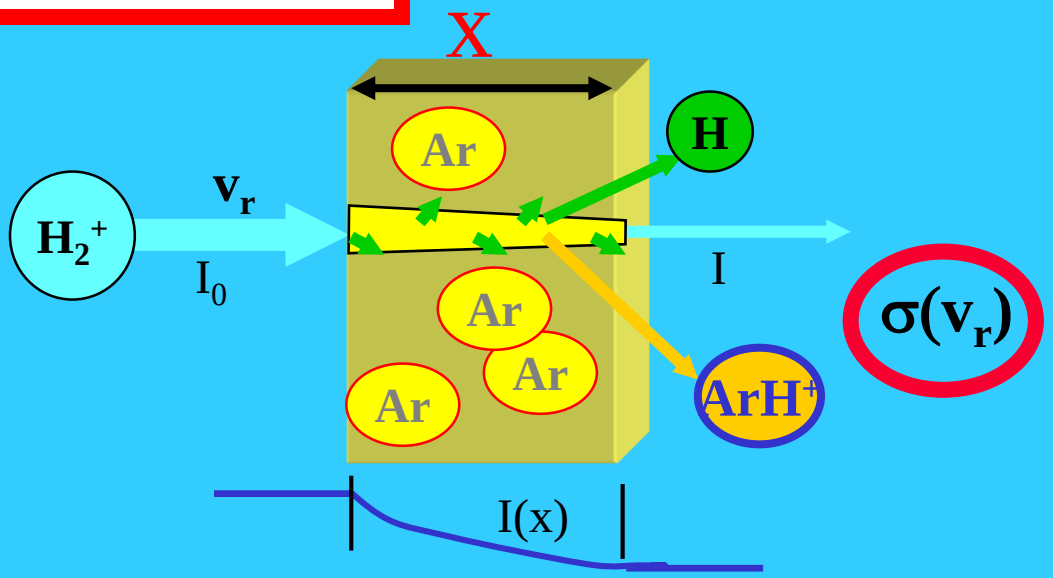

$$I = I_0 \exp(-\sigma n_{Ar} x)$$

$$\nu_{coll} = +nV_{rel} = +n\nu S = +n\nu\pi\delta^2 = +n\nu\sigma$$

Collisional cross section

$$\frac{dI}{dt} = -\frac{I}{\tau_{coll}} = -I\nu_{coll}$$

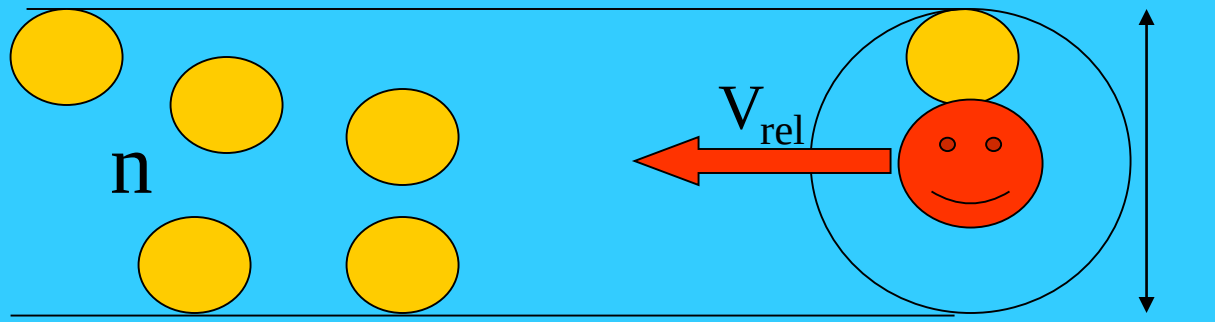

$$I(t) = I_0 \exp(-\nu_{coll} t) = I_0 \exp(-\sigma n \nu_{rel} t)$$

$$I = I_0 \exp(-\sigma n_{Ar} x)$$

Kinetics of elementary process

$$A^+ + B \rightarrow C^+ + D$$

$$\frac{dA^+}{dt} = -k_{BIN} A^+ B$$

$$[A^+]_t = [A^+]_{t=0} \cdot e^{-k[B]t}$$

$$H_2^+ + Ar \Rightarrow ArH^+ + H$$

Multiple collision

@ T

T=T

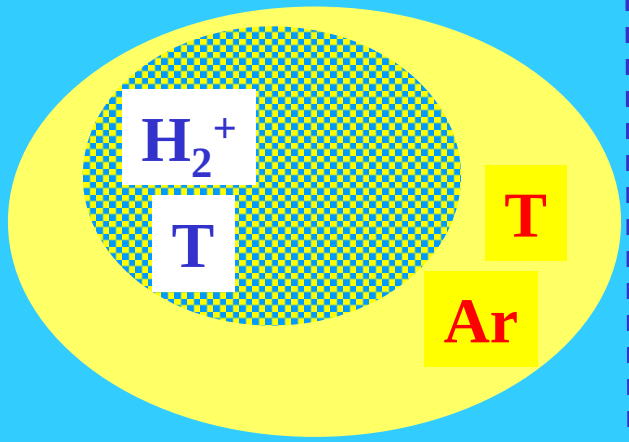

k(T)

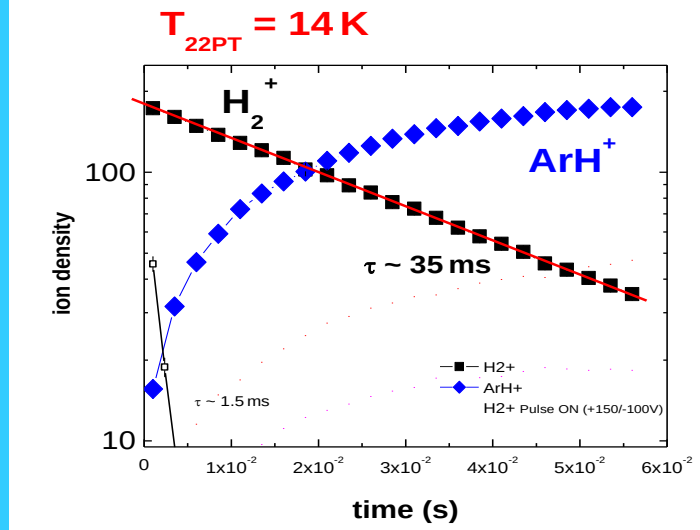

reaction rate coefficient

$d(n_{H2^+})/dt = -k\, n_{H2^+}.\, n_{Ar}$

$n_{H2^+}. = (n_{H2^+})._0 \exp(-k n_{Ar} t)$

Kinetics of elementary process

$$H_2^+ + Ar \Rightarrow ArH^+ + H$$

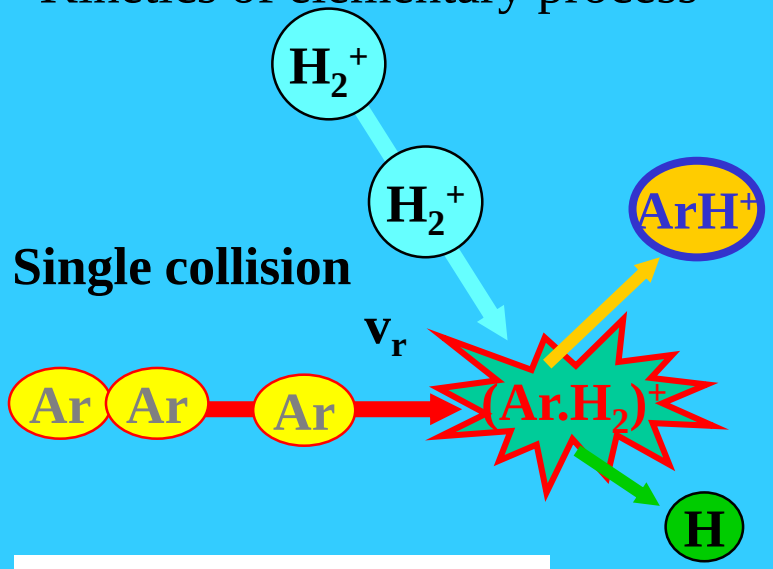

reaction cross section

$$I = I_0 \exp(-\sigma n_{Ar} x)$$

Multiple collision

@ T

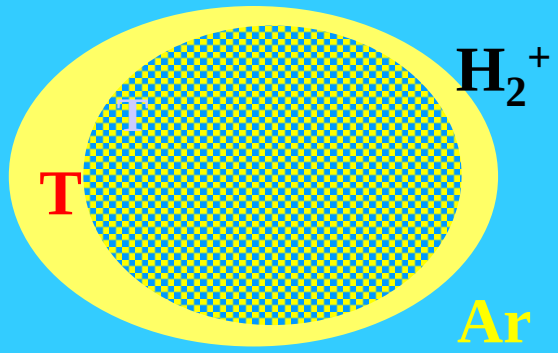

reaction rate coefficient

$$d(n_{H2^+})/dt = -k\, n_{H2^+}.\, n_{Ar}$$

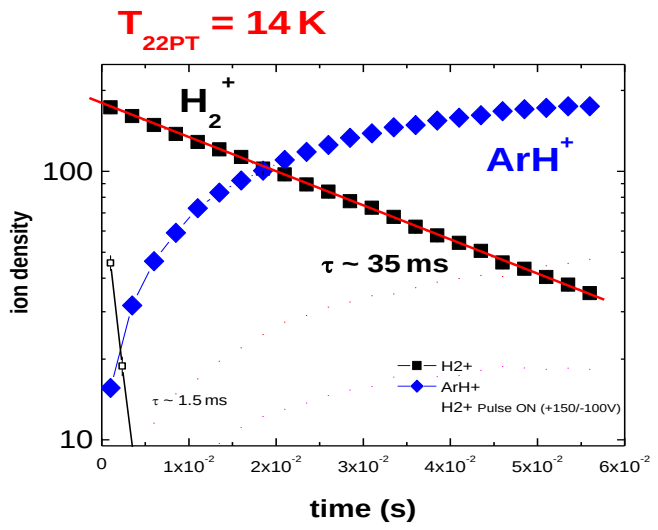

$$n_{H2^+}. = (n_{H2^+}).{}_0 \exp(-k n_{Ar} t)$$

$\sigma(v_r)$

$k(T) = \langle v\sigma \rangle$

$k(T)$

$$A^+ + B \rightarrow C^+ + D$$

$\sigma(v_r)$

$$k_{BIN} = k_{BIN}(T)$$

$$\mathbf{k(T)=<v_r\sigma(v_r)>}$$

$$k = \int_v f_T(v).v.\sigma(v)dv = k(T)$$

Electron scattering cross-section on Ar

$$k = \int_v f_T(v).v.\sigma(v)dv = k(T)$$

Electrons – Boltzman distribution with T_e

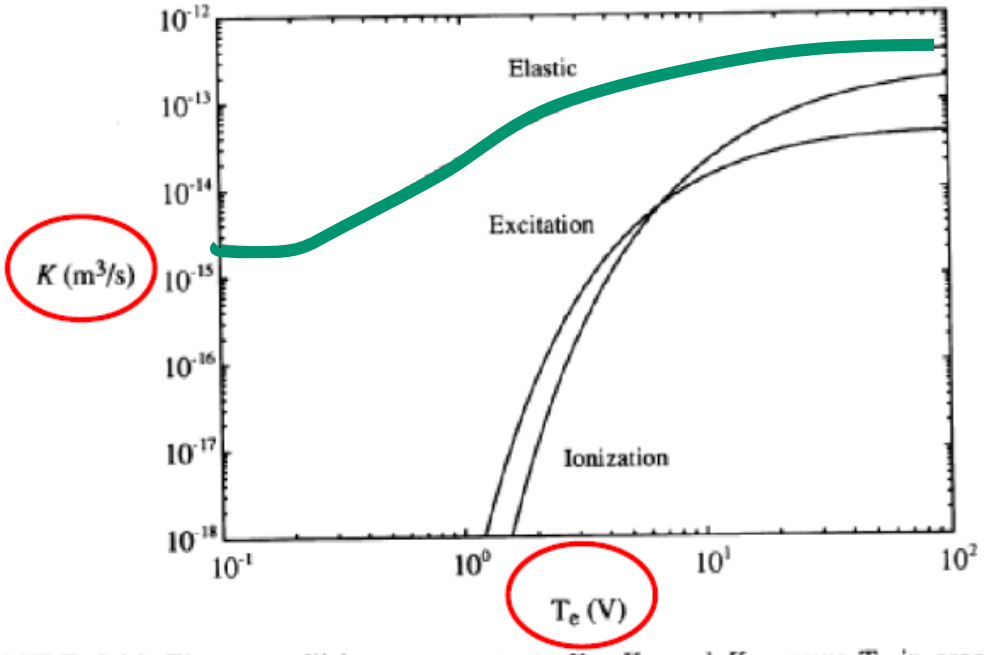

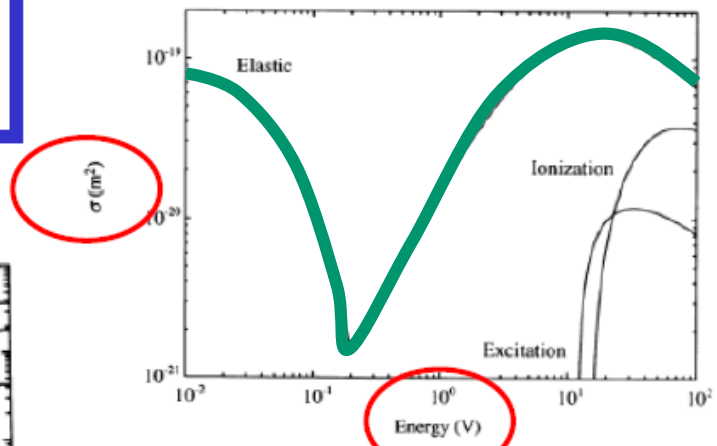

3. Ionization, excitation and elastic scattering cross sections for electrons in
ıpiled by Vahedi, 1993).

$$\alpha(T, T_e) \propto \int_0^\infty \sqrt{E}\,\sigma_w(E,T) f(E,T_e) dE$$

FIGURE 3.16. Electron collision rate constants K_{iz}, K_{ex} and K_m versus T_e in argon gas (compiled by Vahedi, 1993).

What if we have metastables?

Lieberman&Lichtenberg

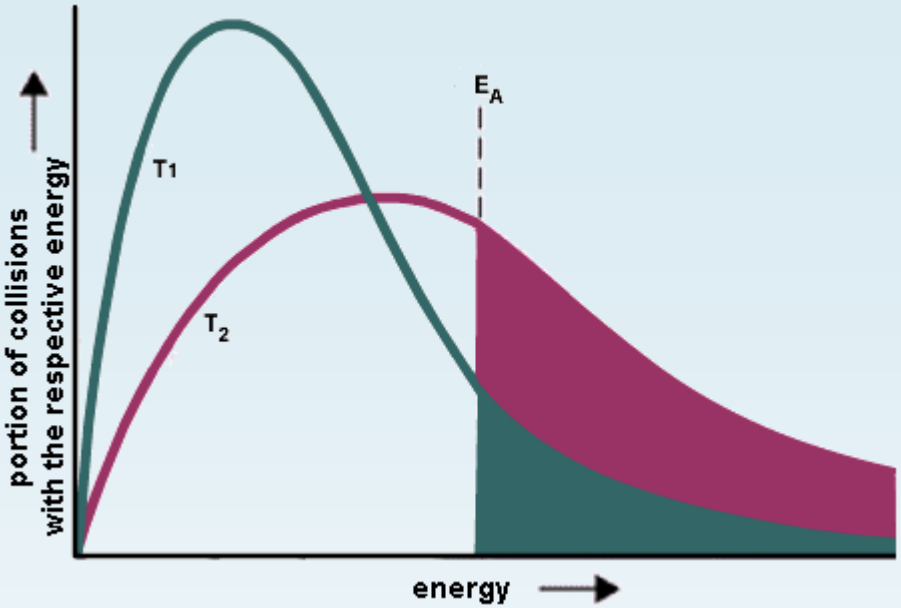
portion of collisions
with the respective energy
E_A
T_1
T_2
energy

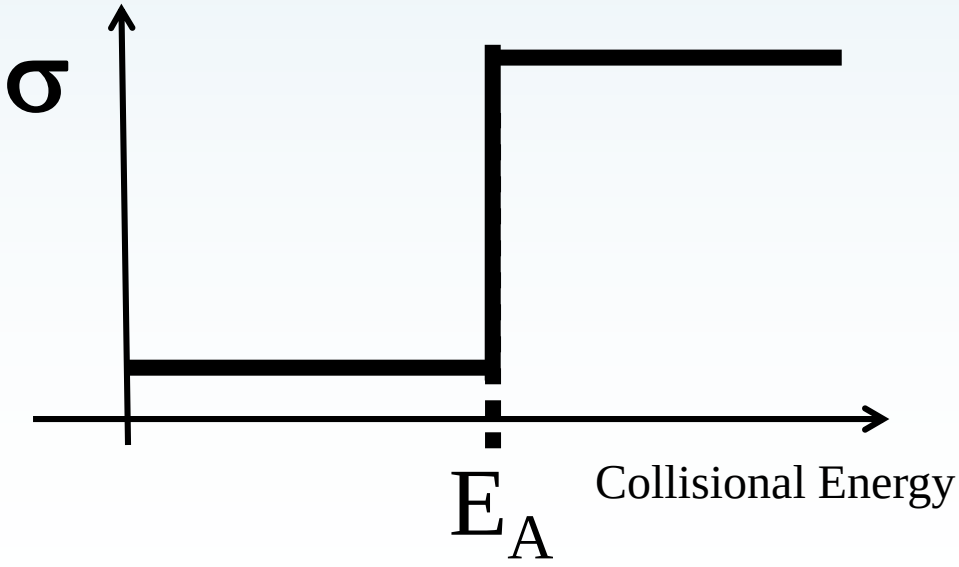
σ
E_A
Collisional Energy

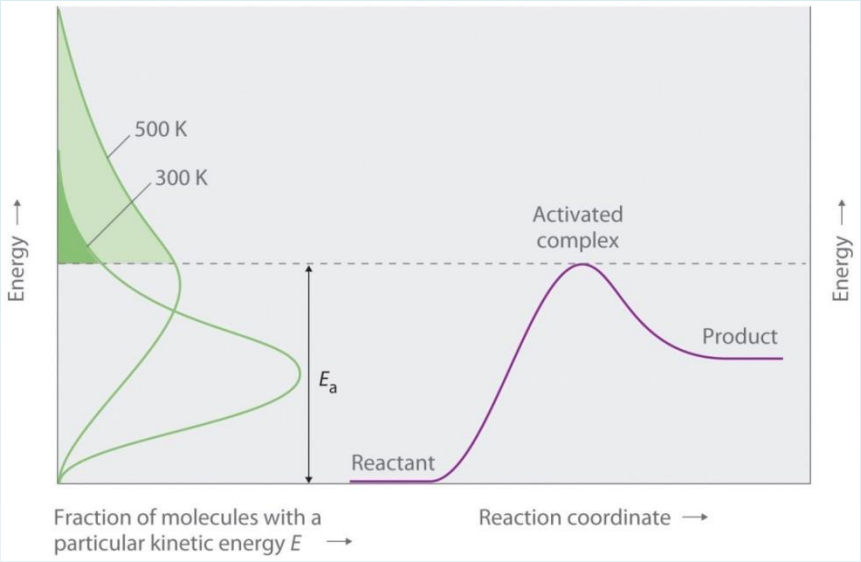

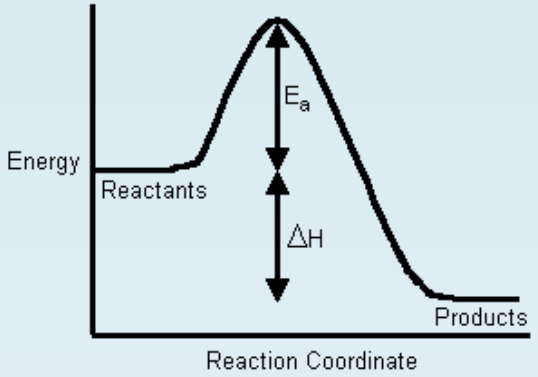

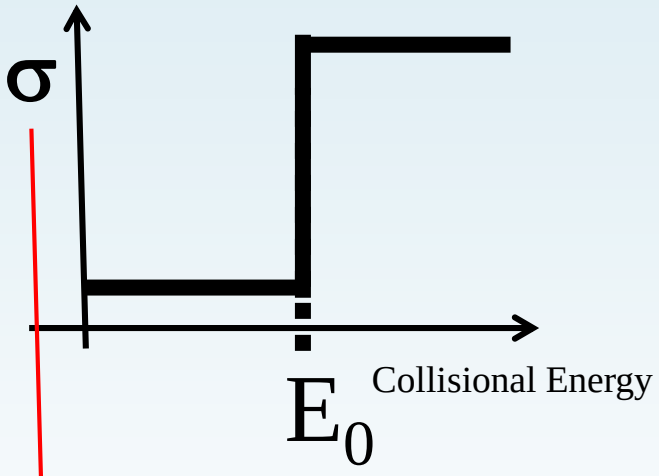

The thermal average rate constant

The thermal average reaction rate constant

The reaction rate coefficient

The thermally averaged rate constant $\alpha_{th}(T)$ (in a.u.) is obtained from the energy-dependent cross-section $\sigma(E)$ as

$$\alpha_{th}(T) = \frac{8\pi}{(2\pi kT)^{3/2}} \int_0^\infty \sigma(E_{el}) e^{-\frac{E_{el}}{kT}} E_{el} dE_{el}, \qquad (4)$$

where T is the temperature. Temperature dependencies $\alpha_{th}(T)$ for different rovibrational transitions $v \rightarrow v'$ obtained using equation (4) are shown in Fig. 3 as solid lines.

It is written for process with electron energy e.g. exciatation by collisions with electrons

Higher temperatures favor products for an endothermic reaction

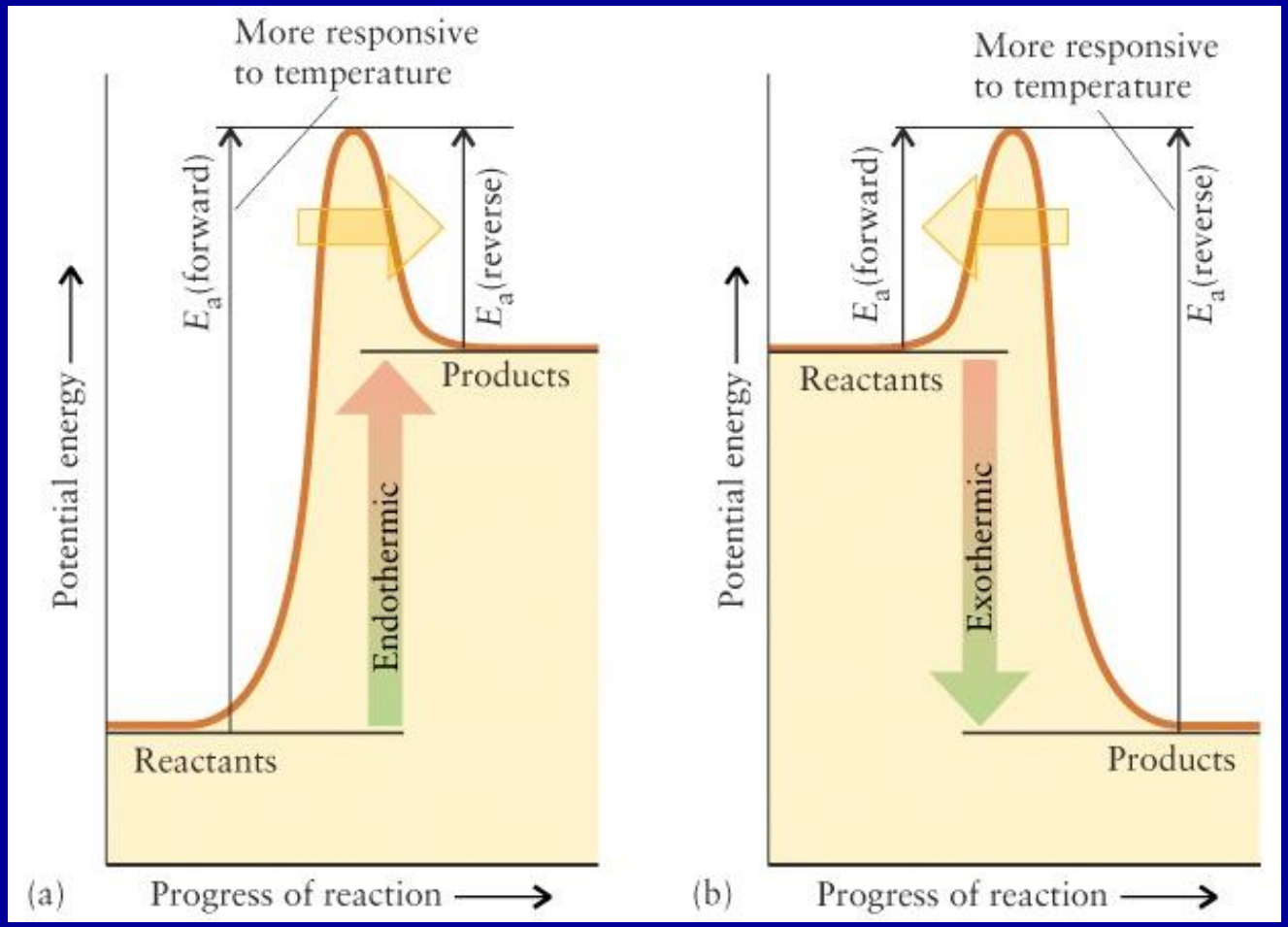

Endothermic reaction: E_a(forward) > E_a(reverse)

Exothermic reaction: E_a(forward) < E_a(reverse)

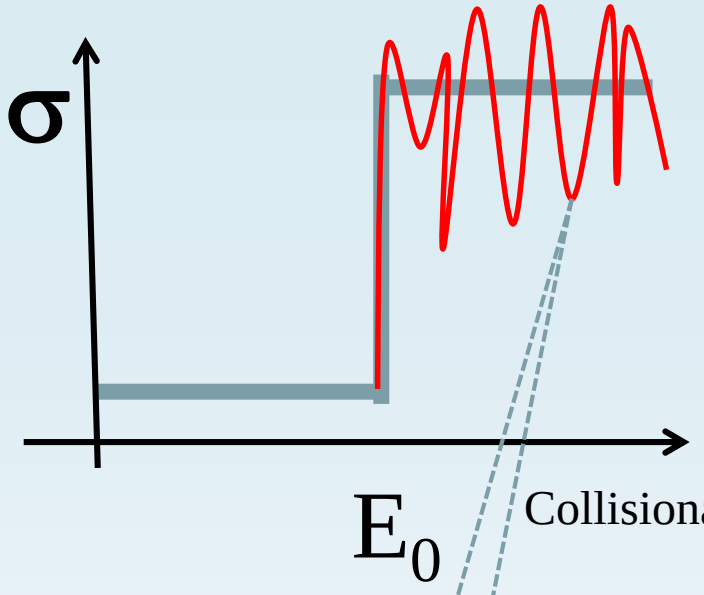

Electron impact rotational excitation of CH⁺

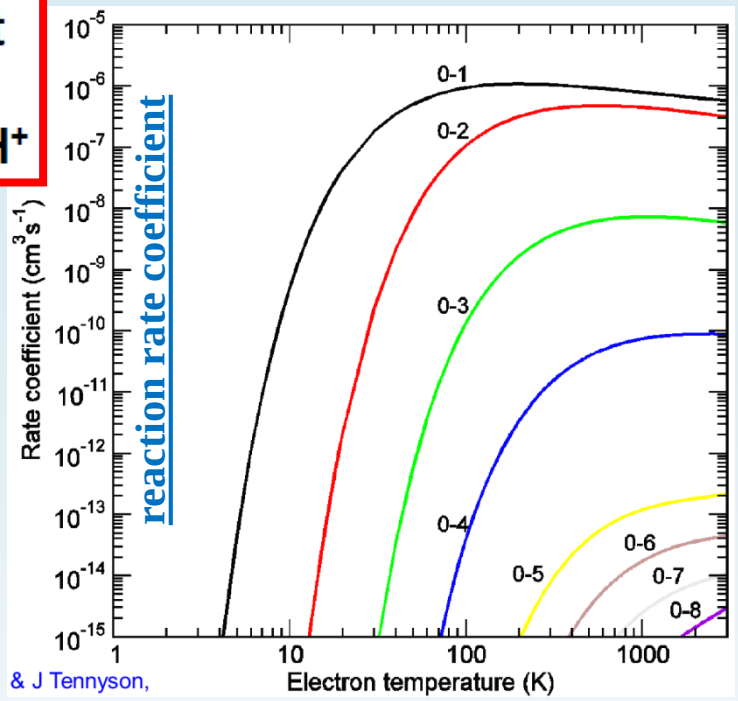

The thermally averaged rate constant $\alpha_{th}(T)$ (in a.u.) is obtained from the energy-dependent cross-section $\sigma(E)$ as

$$\alpha_{th}(T) = \frac{8\pi}{(2\pi kT)^{3/2}} \int_0^\infty \sigma(E_{el}) e^{-\frac{E_{el}}{kT}} E_{el} dE_{el}\,, \qquad (4)$$

where T is the temperature. Temperature dependencies $\alpha_{th}(T)$ for different rovibrational transitions $v \rightarrow v'$ obtained using equation (4) are shown in Fig. 3 as solid lines.

For further discussion, it is convenient to represent the cross-section $\sigma(E_{el})$ in the form

$$\sigma(E_{el}) = \frac{\pi}{k^2} P(E_{el})\,, \qquad (5)$$

where k is the wave vector of the incident electron, $P(E_{el})$ is the probability for vibrational (de-)excitation at collision energy E_{el}.

Arrhenius dependence

$$k = A\, e^{-\frac{E_a}{RT}}$$

activation energy

pre-exponential factor

average kinetic energy

$$\ln k = \ln A - \frac{E_a}{RT}$$

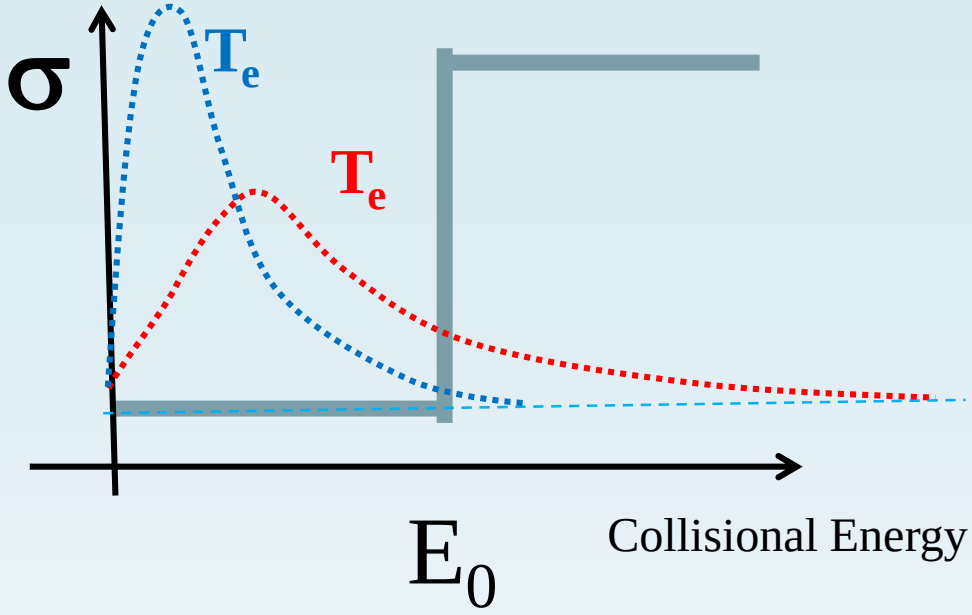

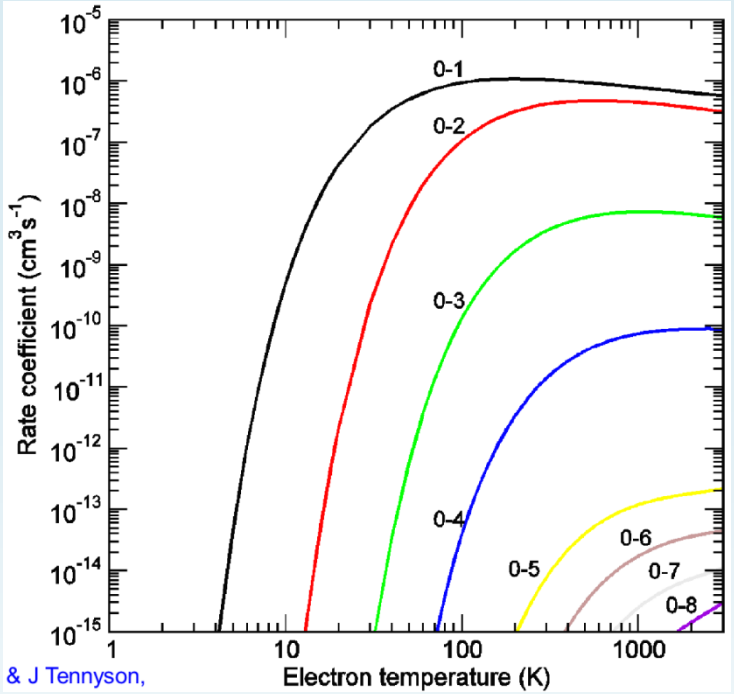

Arrhenius plot

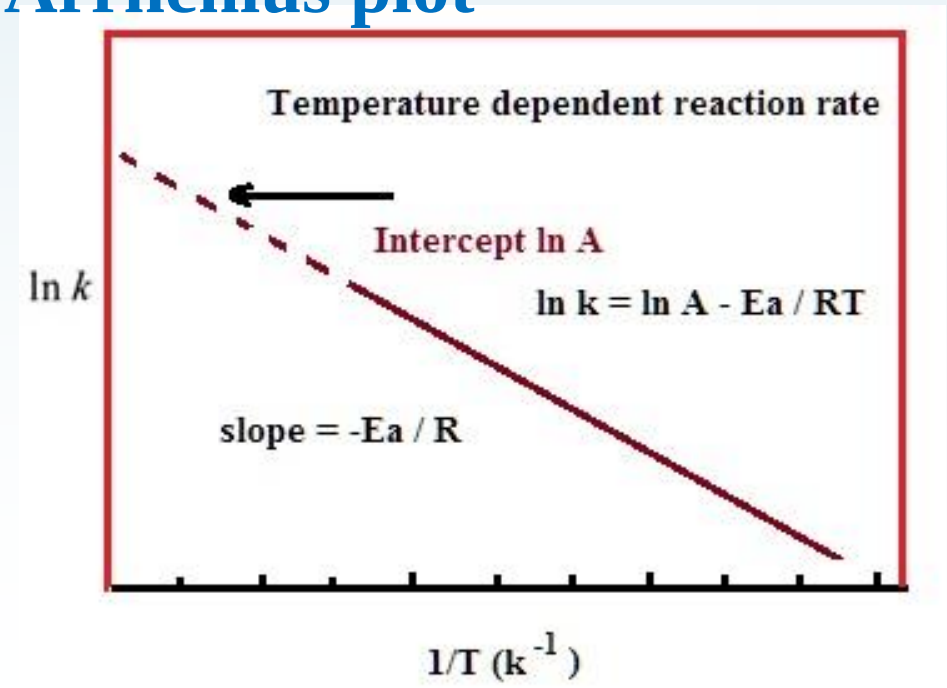

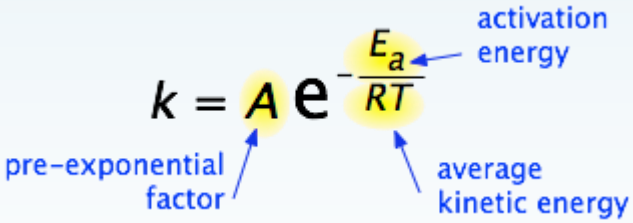

$$\ln k = \ln A - \frac{E_a}{RT}$$

Collision cross section of IMR

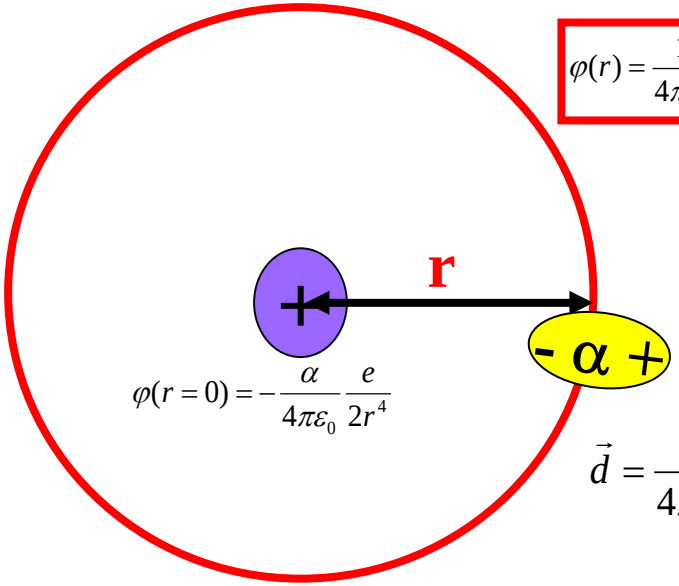

$$\varphi(r) = \frac{1}{4\pi\varepsilon_0}\frac{e}{r}$$

$$\varphi(r=0) = -\frac{\alpha}{4\pi\varepsilon_0}\frac{e}{2r^4}$$

$$\vec{d} = \frac{\alpha}{4\pi\varepsilon_0}\frac{e}{r^2}\frac{\vec{r}}{r}$$

α - polarizability

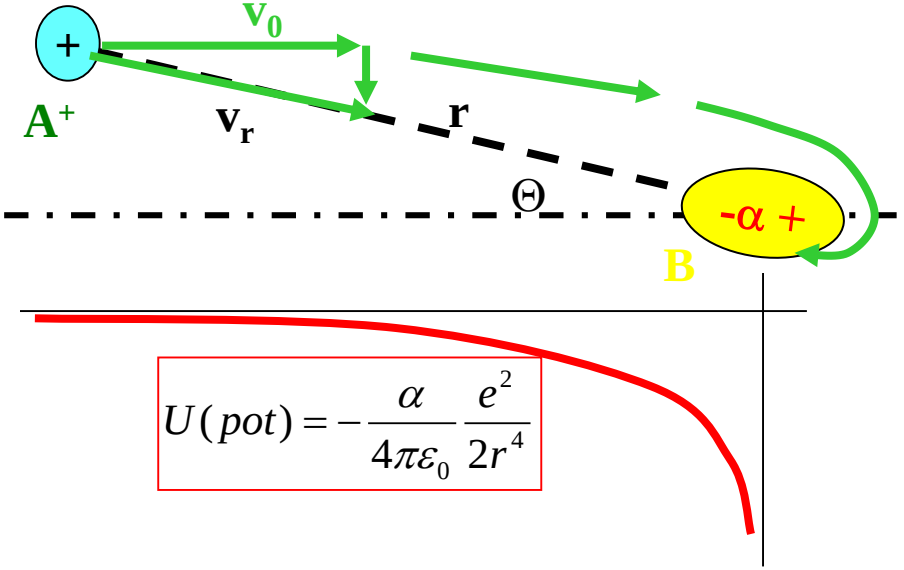

$$U(pot) = -\frac{\alpha}{4\pi\varepsilon_0}\frac{e^2}{2r^4}$$

$$\frac{\mu v_0^2}{2} = \frac{\alpha}{4\pi\varepsilon_0}\frac{e^2}{2r^4}$$

$$\sigma = \pi\rho_0^2 = \frac{2\pi e}{v_0(4\pi\varepsilon_0)}\sqrt{\frac{\alpha}{\mu}}$$

$$\sigma = \pi\rho_0^2 \sim \frac{1}{v_0}\sqrt{\frac{\alpha}{\mu}} \sim \frac{1}{\sqrt{E}}$$

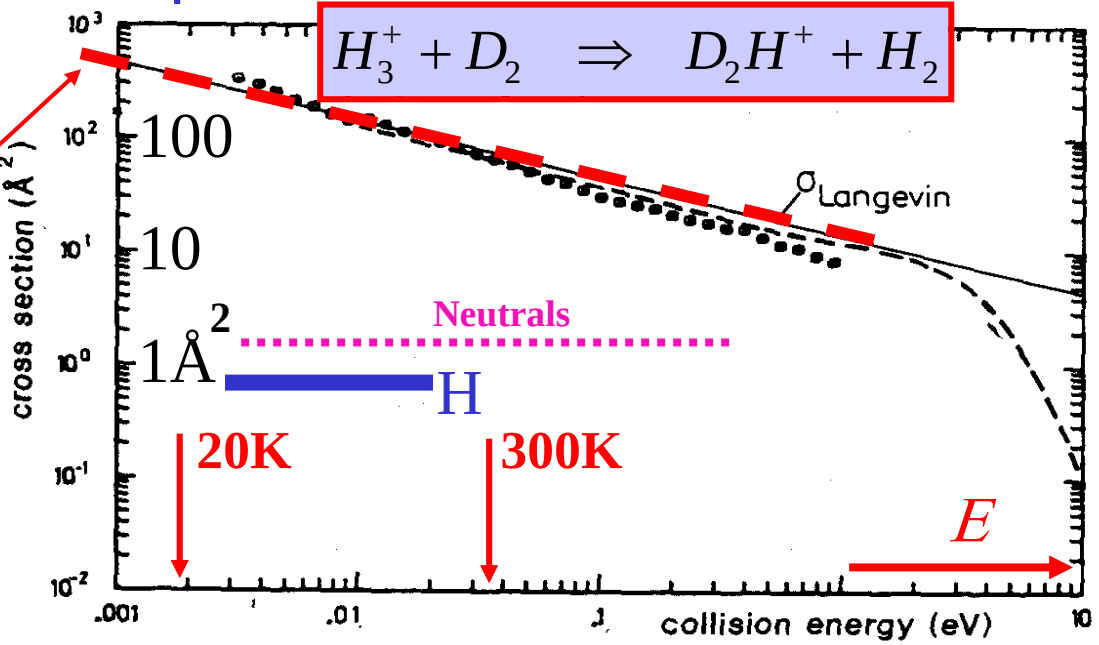

N3+

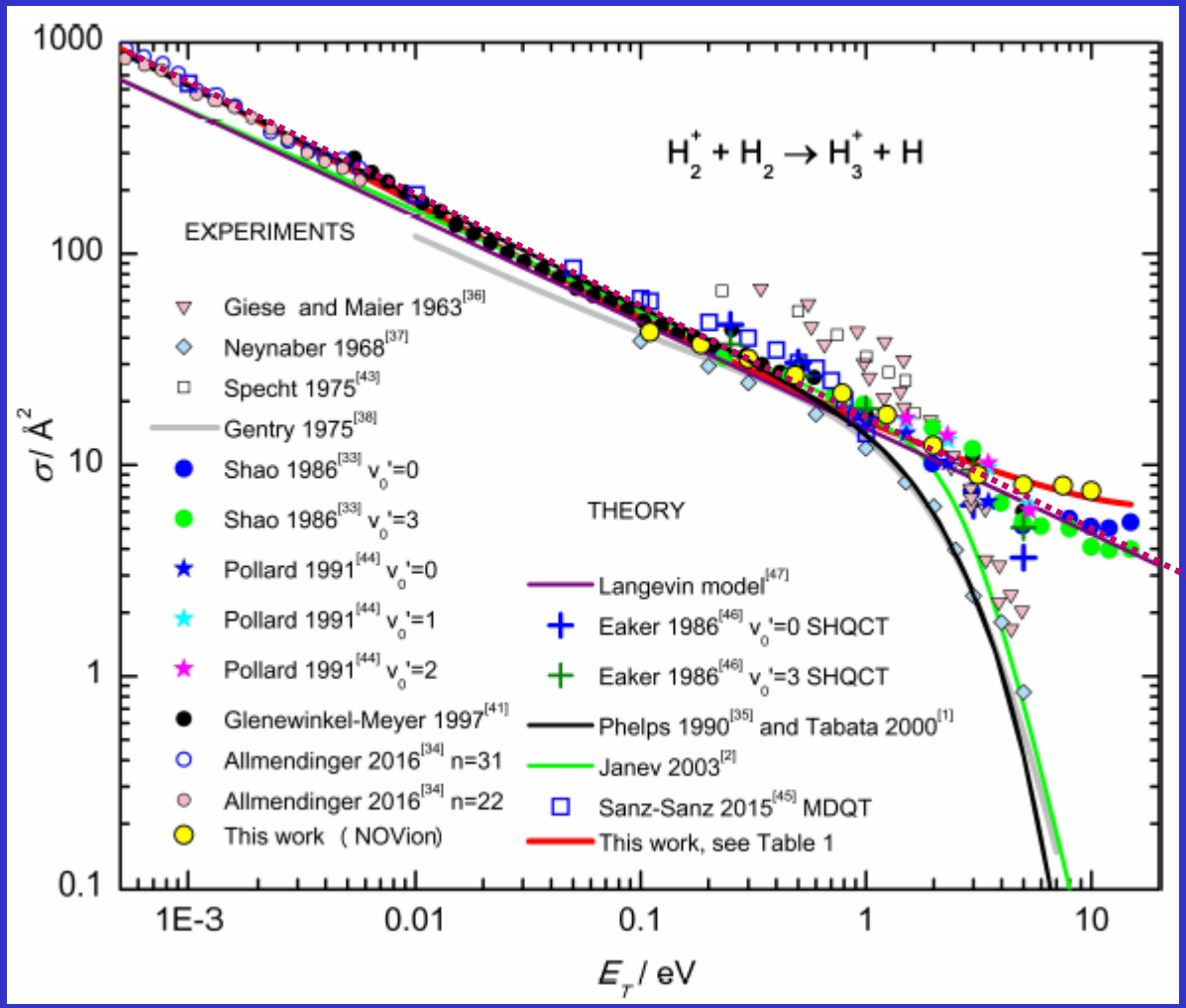

2020

$$H_2^+ + H_2 \rightarrow H_3^+ + H$$

$\sigma_L(E_T)$

$$\sigma = \pi\rho_0^2 \sim \frac{1}{v_0}\sqrt{\frac{\alpha}{\mu}} \sim \frac{1}{\sqrt{E}}$$

Langevin

Figure 2. Dependence of the integral cross section for the reaction $H_2^+ + H_2 \rightarrow H_3^+ + H$ on the collision energy E_T. In the meV and sub-meV energy range, there is good agreement between two different merged beam results, Refs. [34,41]. Note that Allmendinger et al.[34] scaled their relative cross sections to the absolute ones calculated by Sanz-Sanz et al.[45] as described in the caption of figure 10 of Ref. [34]. Between thermal energies and 1 eV, most of the published and tabulated values agree more or less with the function proposed in the compilations by Tabata[1] (black line) and Janev et al.[2] (green line). However, based on results from the sixties and seventies, a steep decline has been predicted above 2 eV. In contrary, our results (yellow filled circles) do not show this trend, in accordance with the guided ion beam results from Shao et al.[33] The data presented in Ref. [35] as tabulated values and in Ref. [1] as an analytical function are nearly identical and are represented here simply by the one black line.

IMR thermal

$$\sigma = \pi\rho_0^2 = \frac{2\pi e}{v_0(4\pi\varepsilon_0)}\sqrt{\frac{\alpha}{\mu}}$$

$$k = \int_v f_T(v).v.\sigma(v)dv = k(T)$$

$k_{col} = \langle v\rho \rangle \sim \langle v.1/v \rangle = \text{const.}$

$k_{coll} \sim 10^{-9} cm^3 s^{-1}$

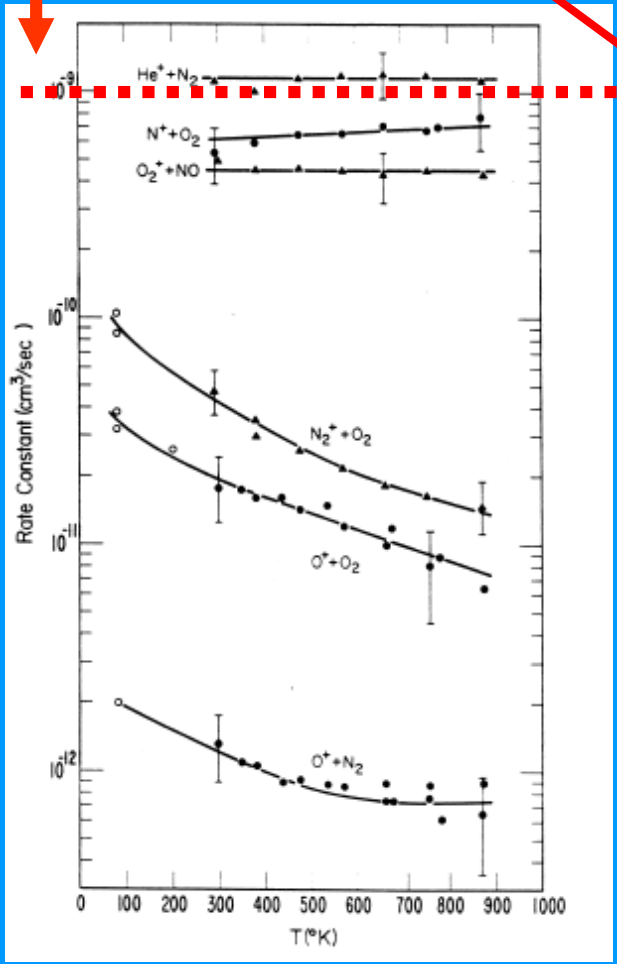

Ionic composition of the atmosphere

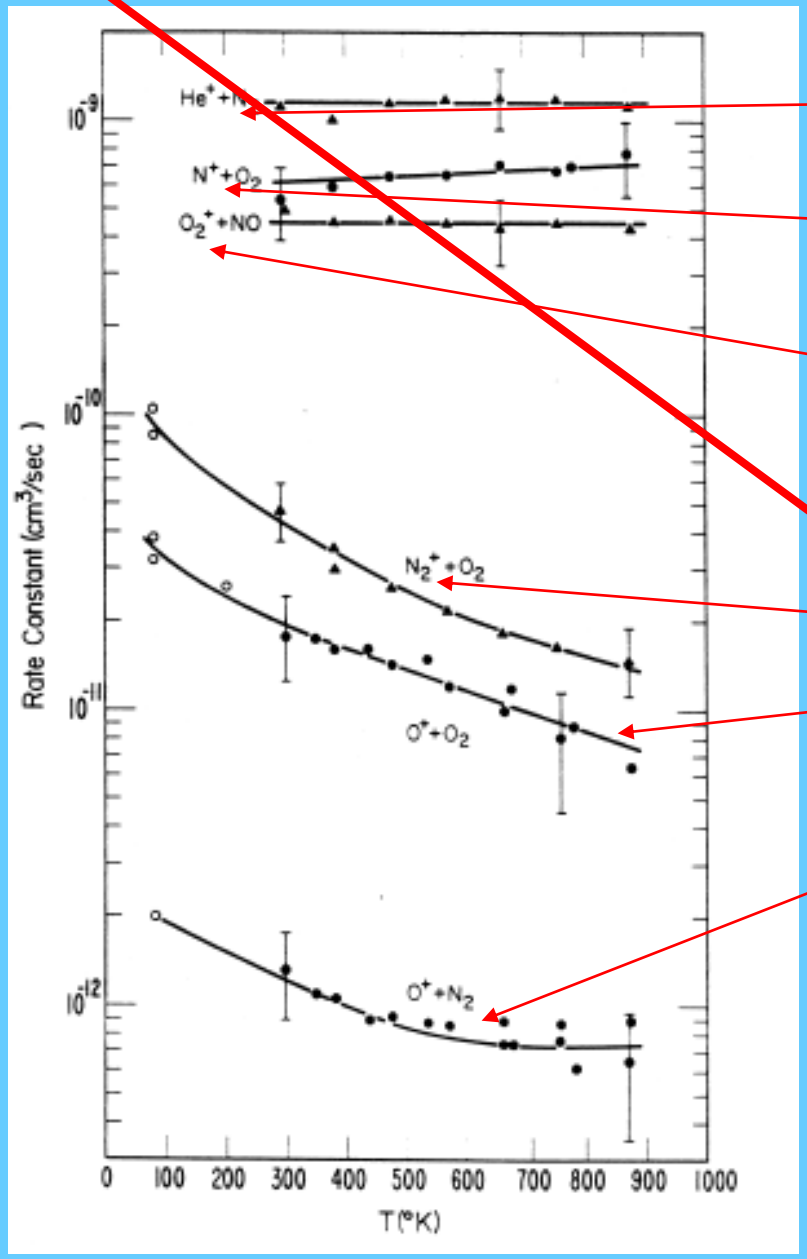

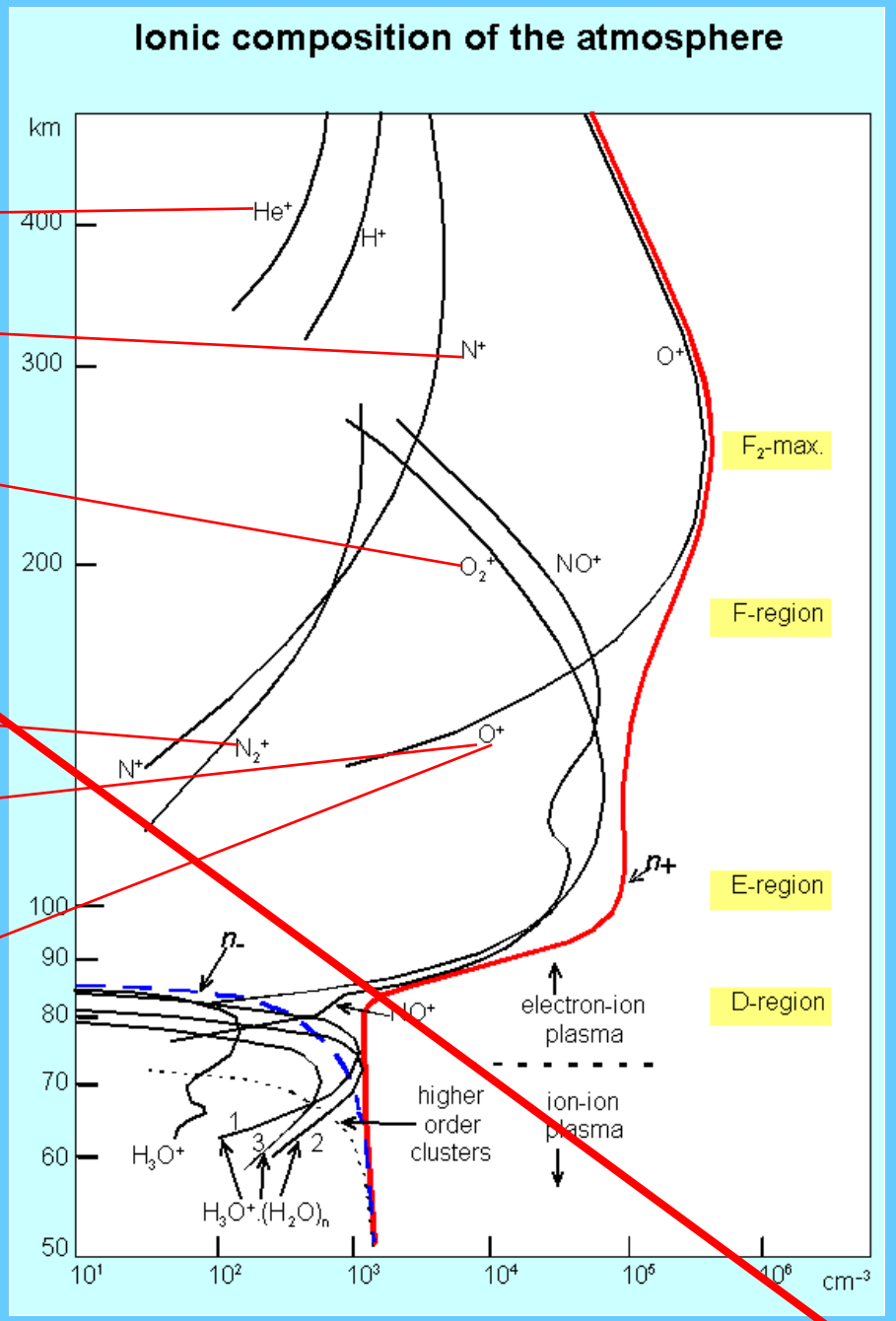

Reaction Rate of IMR relevant for ionosphere

k_{IMR}

$k_{coll} \sim 10^{-9} cm^3 s^{-1}$

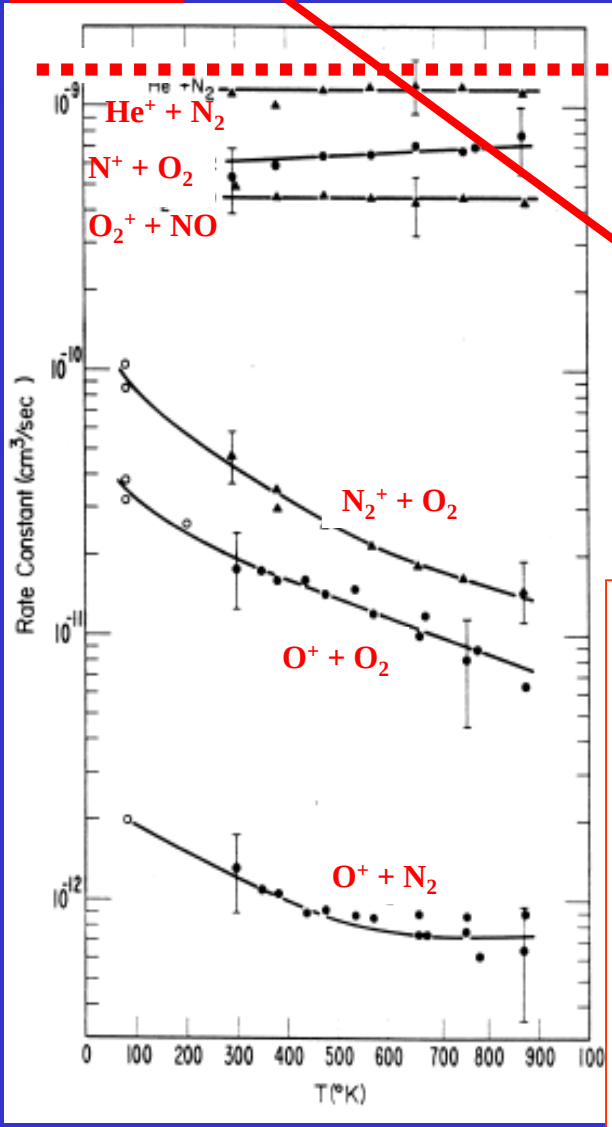

1975-90

k_{IMR}

1990-00

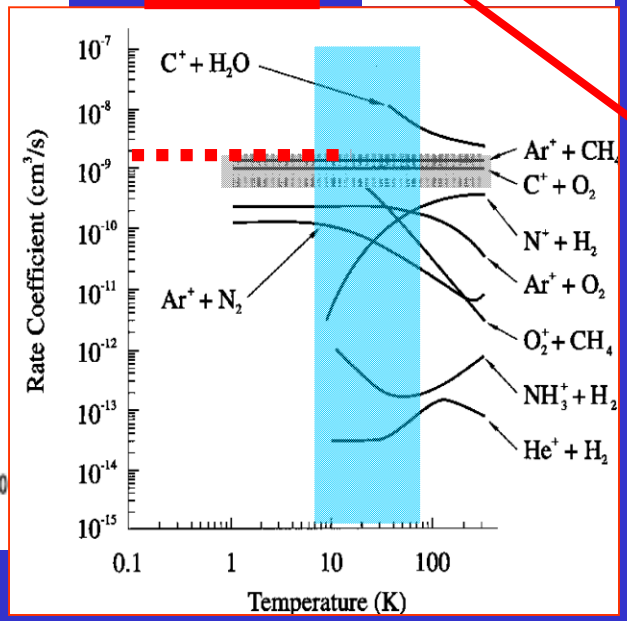

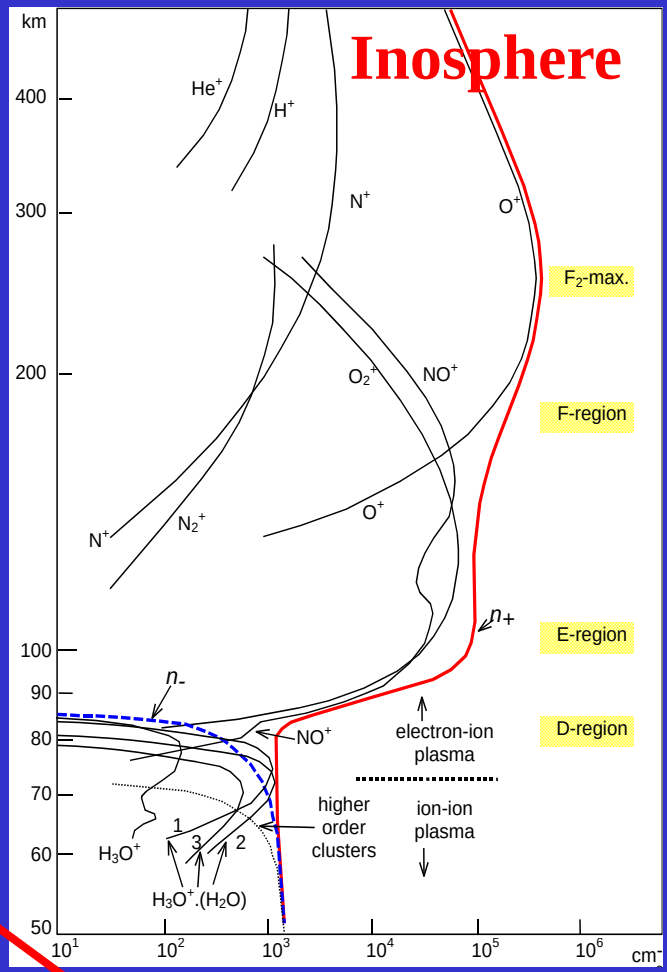

Interactions of electron
Rotational and vibrational excitation

Rutherford atom

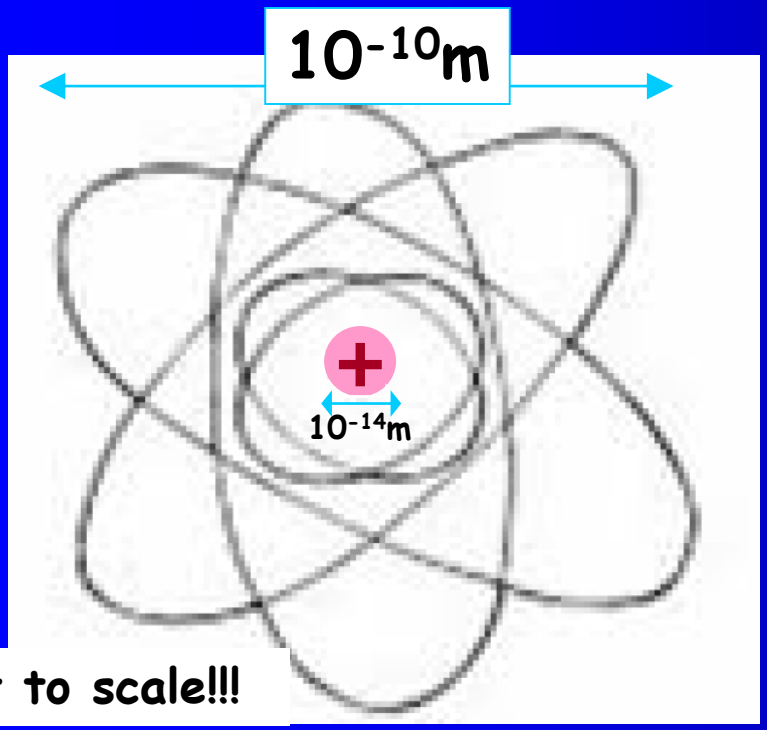

Excitation energies

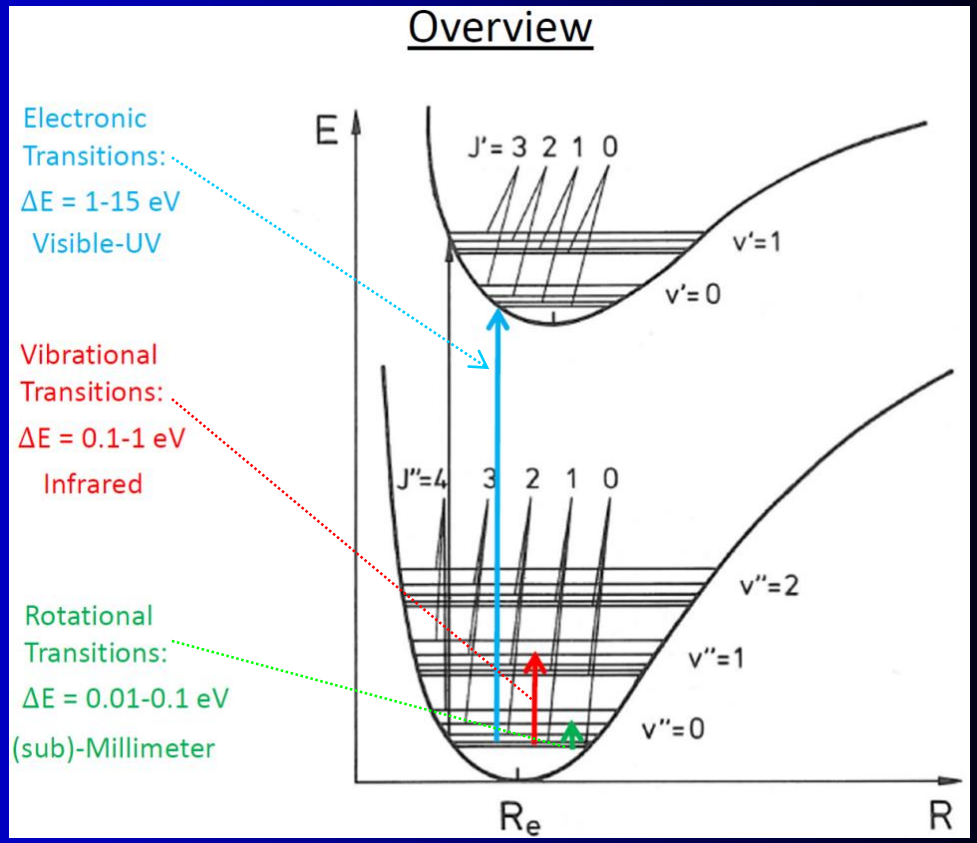

Electron: 1eV → v=5.9x10^{7}cm s^{-1}

$\tau \sim a_0/v \sim 10^{-8}/ 5.9x10^7 = 2x10^{-16}$s

Energy levels

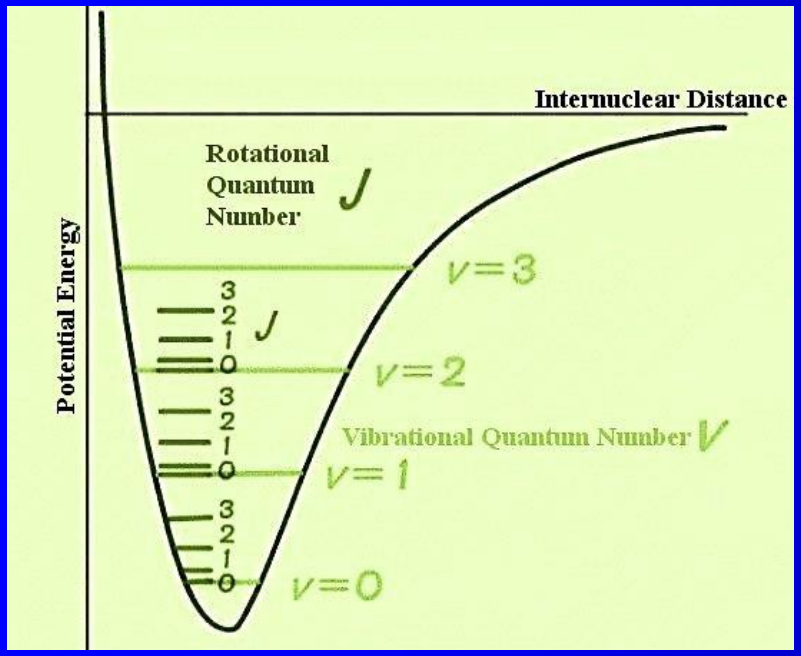

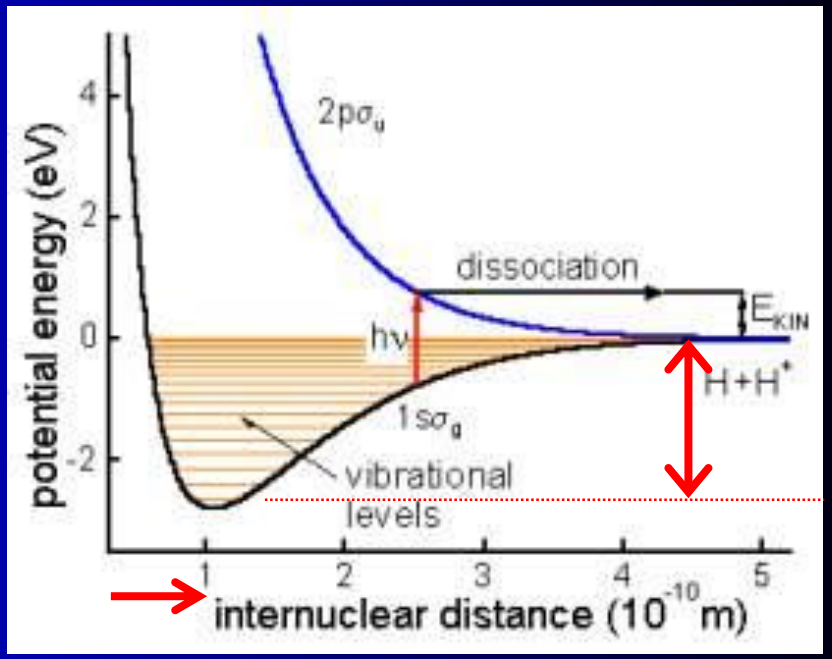

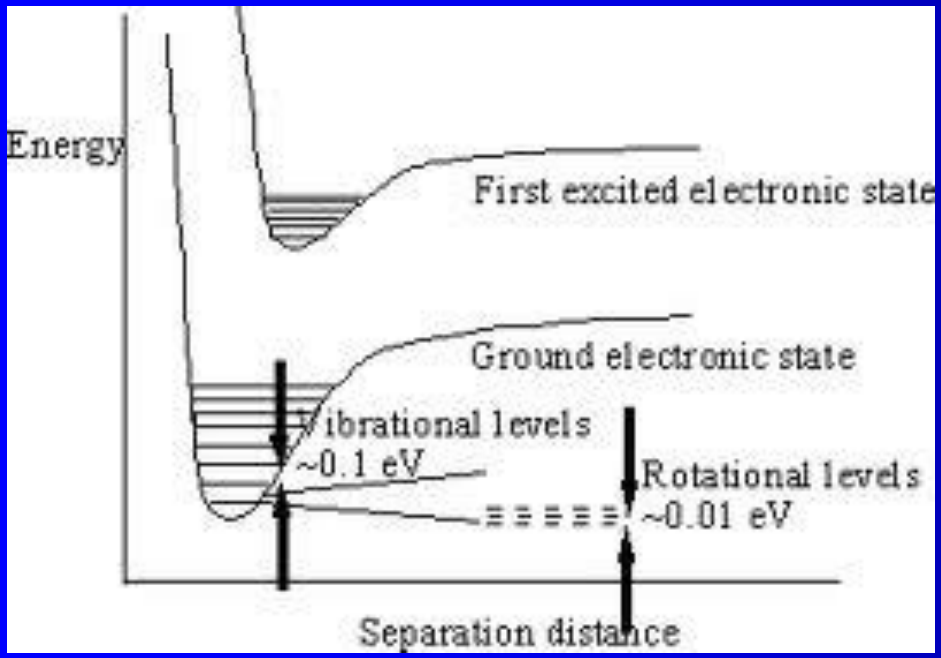

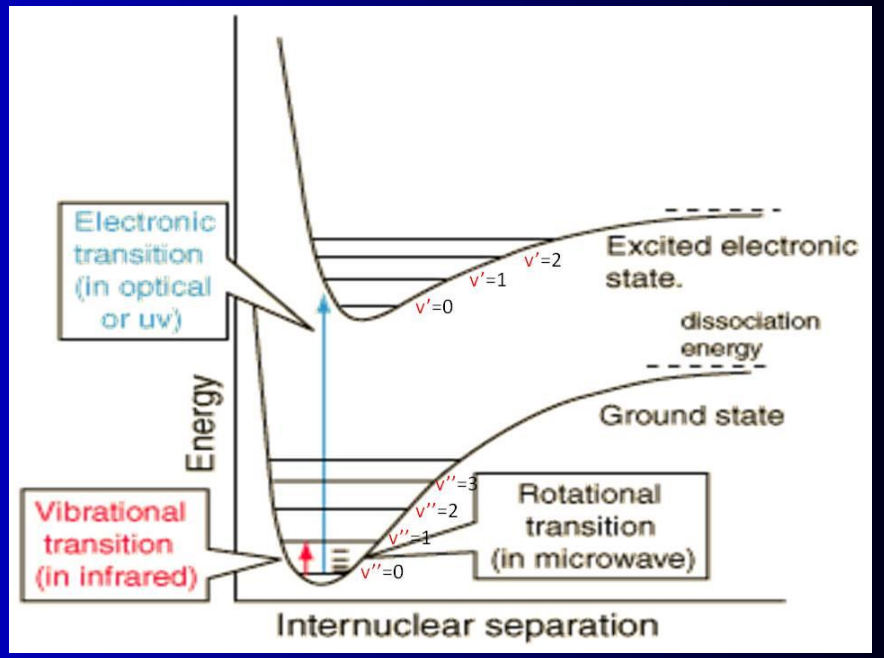

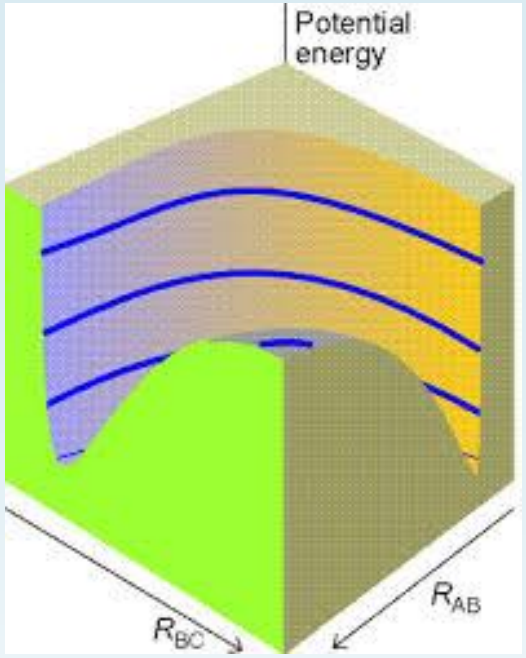
Potential
energy
R_{BC}
R_{AB}

H-C + D ➔ H C D ➔ H + C-D
H + C
H⇔C
Energy Surface for H-C + D ⟺ H + C-D
1 < x < 10 A, 1 < y < 8 A
H⇔C
Press
N New Start
S Repeat Start
<CR> End Program
8.0
R(DC)
1.0
1.0
R(CH)
10.0
D + C
D
H
C⇔D

Chapter 22: Reaction Dynamics

- **saddle point,** the highest point on a potential energy surface encountered along the reaction coordinate.

$$H_A + H_B\text{-}H_C \rightarrow H_A\text{-}H_B + H_C$$

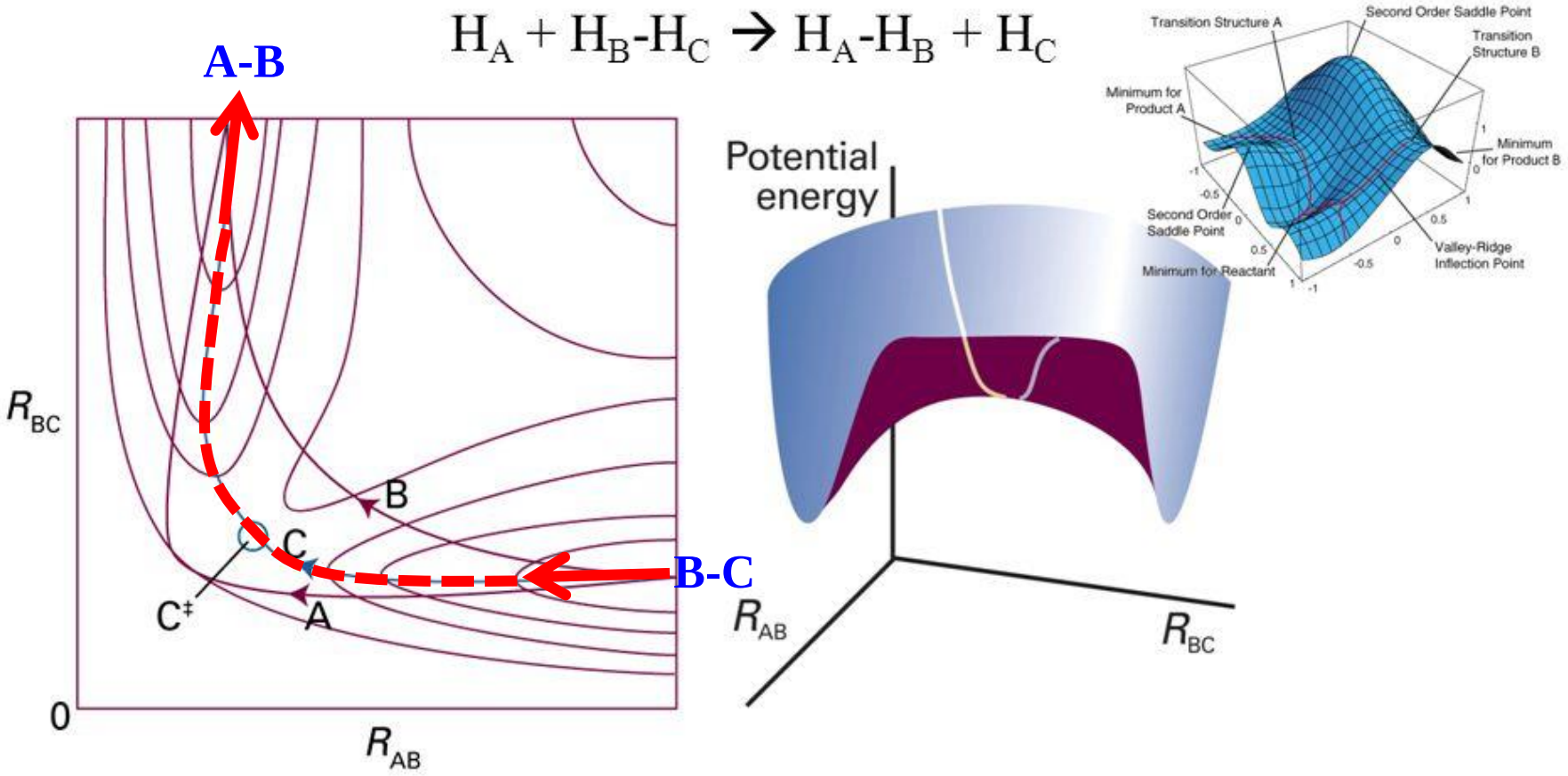

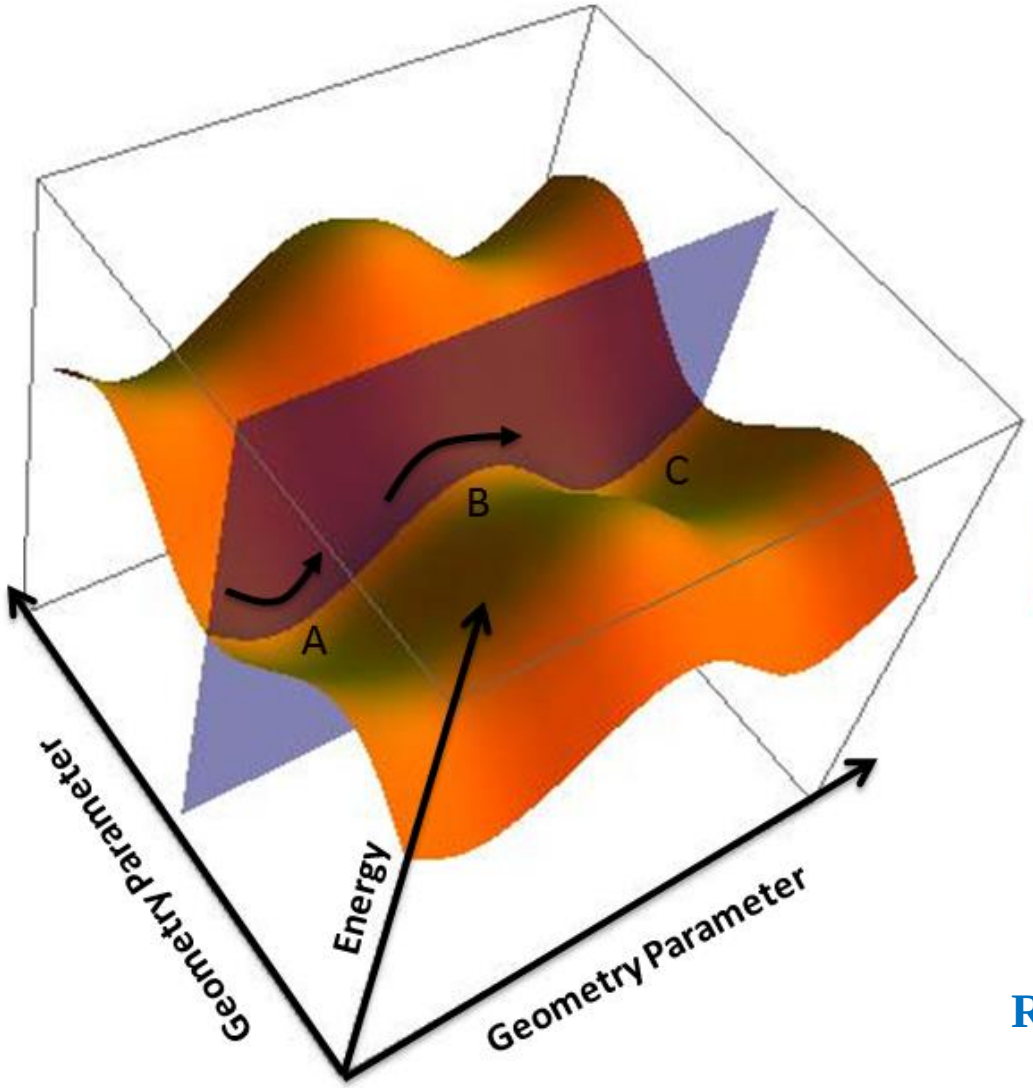

Reaction coordinate

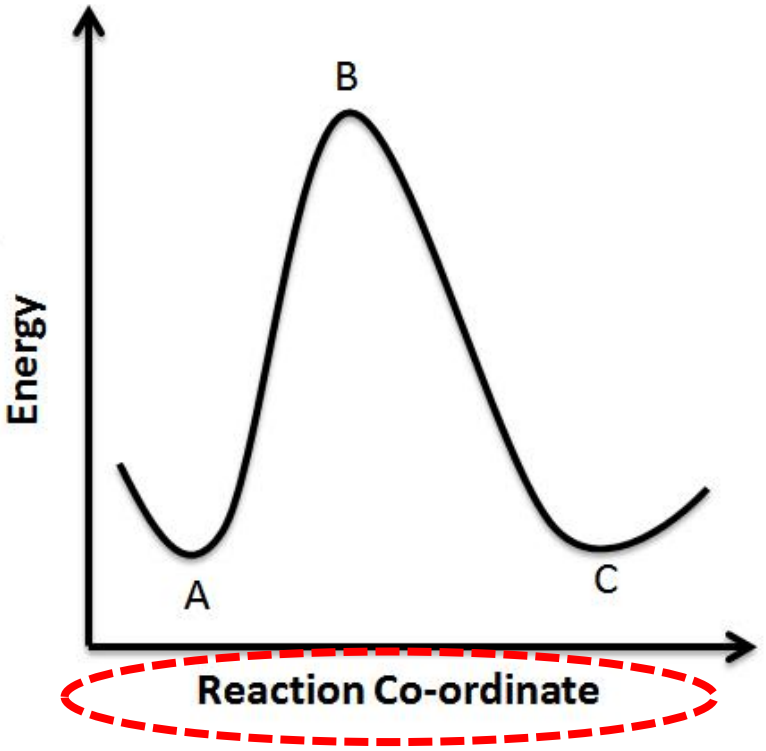

Reaction Coordinate

"…..In chemistry, a **reaction coordinate** is an abstract one-dimensional coordinate which represents progress along a reaction pathway. It is usually a geometric parameter that changes during the conversion of one or more molecular entities. In molecular dynamics simulations, a reaction coordinate is called **collective variable**. ….."

$$A + H_2 \rightarrow \ldots. \rightarrow C + \ldots..$$

THE JOURNAL OF PHYSICAL CHEMISTRY A
Article
pubs.acs.org/JPCA

Accurate Time-Dependent Wave Packet Calculations for the $O^+ + H_2 \rightarrow OH^+ + H$ Ion–Molecule Reaction

N. Bulut,[†] J.F. Castillo,[‡] P. G. Jambrina,[‡] J. Klos,[§] O. Roncero,[∥] F. J. Aoiz,[‡] and L. Bañares*[,‡]

J. Phys. Chem. A 2015, 119, 11951–11962

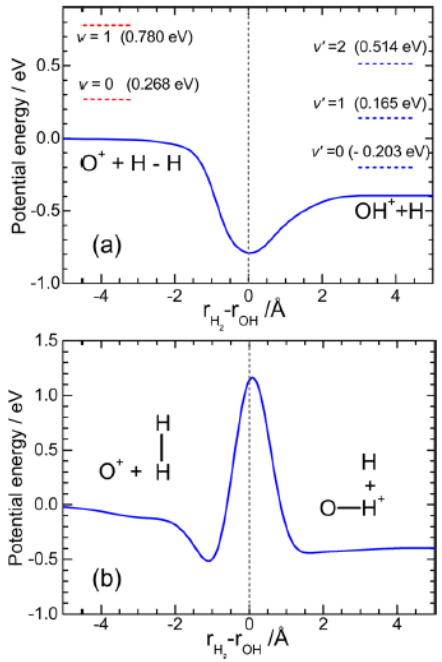

Figure 1. Minimum energy path for the $O^+ + H_2 \rightarrow OH^+ + H$ reaction calculated on the MMG PES[10] as a function of $r_{H_2} - r_{OH}$. (a) Collinear configuration, $\widehat{OHH}$ angle $\alpha = 180°$. The dashed horizontal lines indicate the energy of the initial H_2 $v = 0$ and $v = 1$, and final OH^+ $v' = 0$, $v' = 1$, and $v' = 2$ vibrational states. (b) Perpendicular configuration $\widehat{OHH}$ angle $\alpha = 90°$.

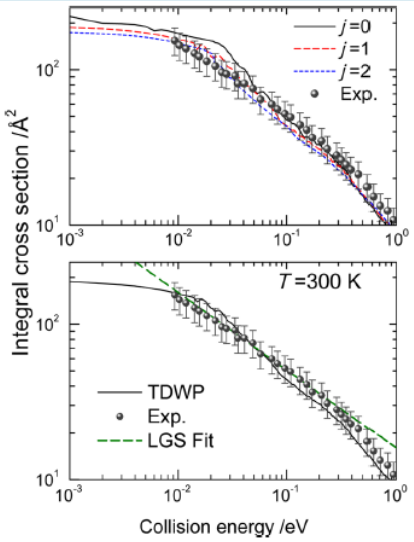

Figure 8. Top: total reaction cross section as a function of collision energy for the $O^+ + H_2(v=0,j)$ reactions. Solid black line: $j = 0$. Red dashed line: $j = 1$. Blue short-dashed line: $j = 2$. Solid circles: experimental results from ref 7. Bottom: Total reaction cross section as a function of collision energy for the $O^+ + H_2(v=0,\langle j \rangle)$ reaction averaged over the thermal rotational population at 300 K. Black solid line: TDWP. Solid circles: experimental results from ref 7. Green dashed line: Langevin model, $\sigma_r(E_c) = AE_c^{-1/2}$; $A = 16$ Å^2 eV$^{1/2}$.

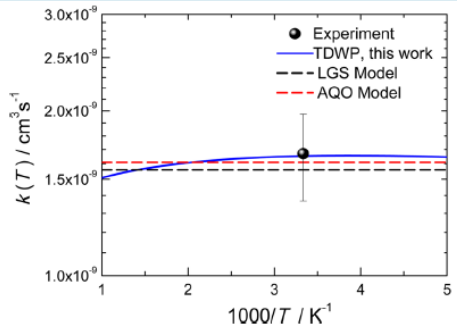

Figure 9. Thermal rate constants for the $O^+ + H_2$ reaction. Blue solid line: TDWP. Solid circle: experimental result from ref 7. Black dashed line: Langevin model. Red dashed line: AQO model.

Reaction Coordinate Diagrams

" ……We can follow the progress of a reaction on its way from reactants to products by graphing the energy of the species versus the reaction coordinate. We will be vague in describing the reaction coordinate because its definition is a mess of other variables composed to best make sense of the progress of the reaction. The value of the reaction coordinate is between zero and one. Understanding the meaning of the reaction coordinate is not important, just know that small values of reaction coordinate (0-0.2) mean little reaction has taken place and large values (0.8-1.0) mean that the reaction is almost over. It is a kind of scale of the progress of a reaction. A typical reaction coordinate diagram for a mechanism with a single step is shown below: ….."

Dynamics studies of $O^+ + D_2$ reaction using the time-dependent wave packet method

2019

Ziliang Zhu[a,b], Li Li[b], Qiju Li[b] and Bing Teng[a]

[a]College of Physics, Qing dao University, Qing dao, People's Republic of China; [b]Shandong Peninsula Engineering Research Center of Comprehensive Brine Utilization, Weifang University of Science and Technology, Shouguang, People's Republic of China

ABSTRACT

Based on the potential energy surface (PES) reported by Li *et al.* (Phys. Chem. Chem. Phys. **20**, 1039 (2018)), the initial state dynamics calculation of $O^+ + D_2$ ($v = 0, j = 0$) reaction was conducted using the time-dependent wave packet method with a second order split operator. Dynamics properties such as reaction probability, integral cross section, differential cross section, and distribution of products were calculated and compared with available experimental and theoretical results. The present integral cross section values were in good agreement with experimental results. In addition, the differential cross section indicates that the mechanism of the complex-formation reaction plays a dominant role during the reaction.

ARTICLE HISTORY
Received 15 November 2018
Accepted 7 May 2019

KEYWORDS
Reaction probability; $O^+ + D_2$ reaction; integral cross section; time-dependent wave packet

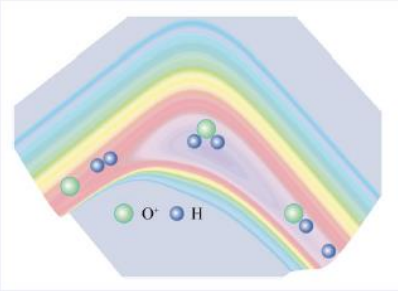

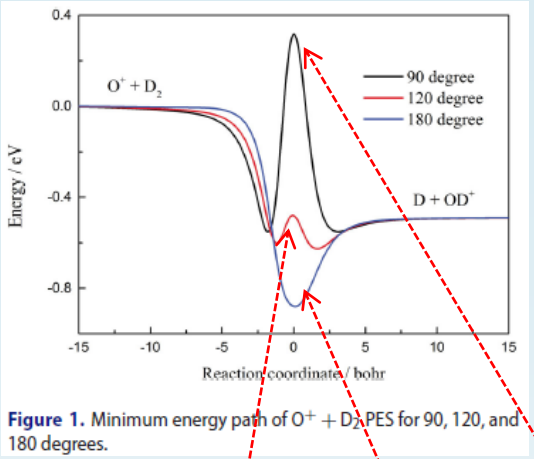

Figure 1. Minimum energy path of $O^+ + D_2$ PES for 90, 120, and 180 degrees.

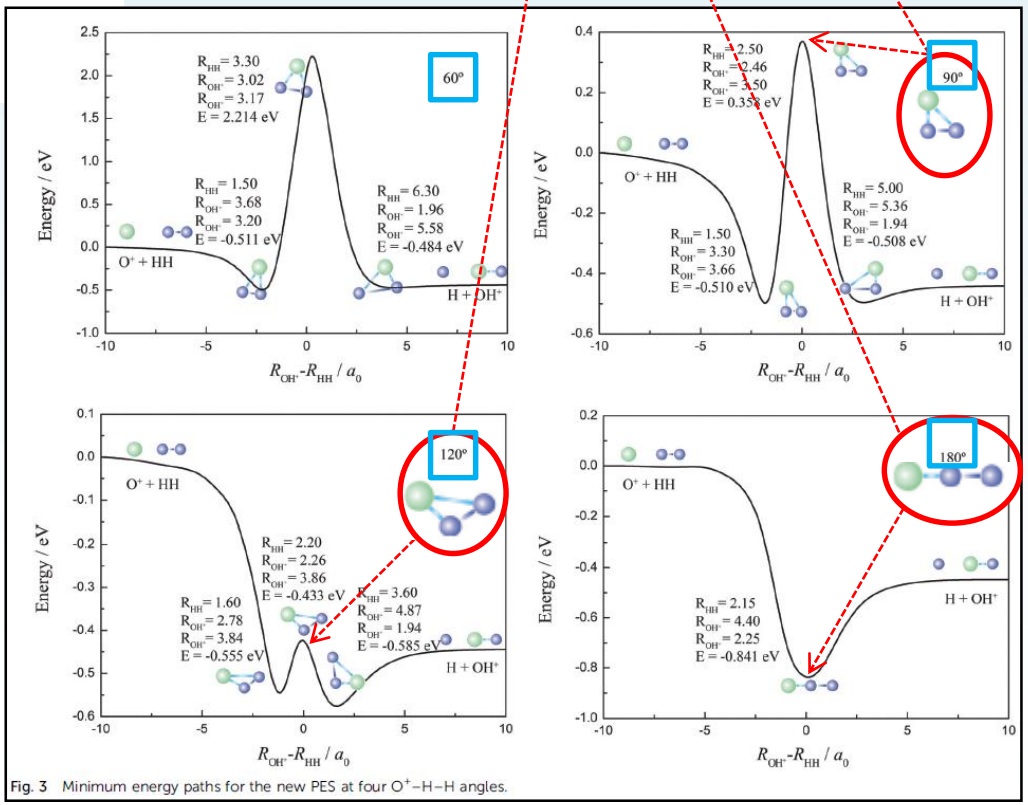

Fig. 3 Minimum energy paths for the new PES at four O^+–H–H angles.

"…..In chemistry, a **reaction coordinate**[1] is an abstract one-dimensional coordinate which represents progress along a reaction pathway. It is usually a geometric parameter that changes during the conversion of one or more molecular entities. In molecular dynamics simulations, a reaction coordinate is called **collective variable**.[2] ….."

Reaction Coordinate

PCCP

PAPER

View Article Online
View Journal | View Issue

Check for updates

Cite this: Phys. Chem. Chem. Phys., 2018, 20, 1039

A new potential energy surface of the OH_2^+ system and state-to-state quantum dynamics studies of the $O^+ + H_2$ reaction†

Wentao Li,[a] Jiuchuang Yuan,[b] Meiling Yuan,[c] Yong Zhang,[d] Minghai Yao[a] and Zhigang Sun*[b]

2018

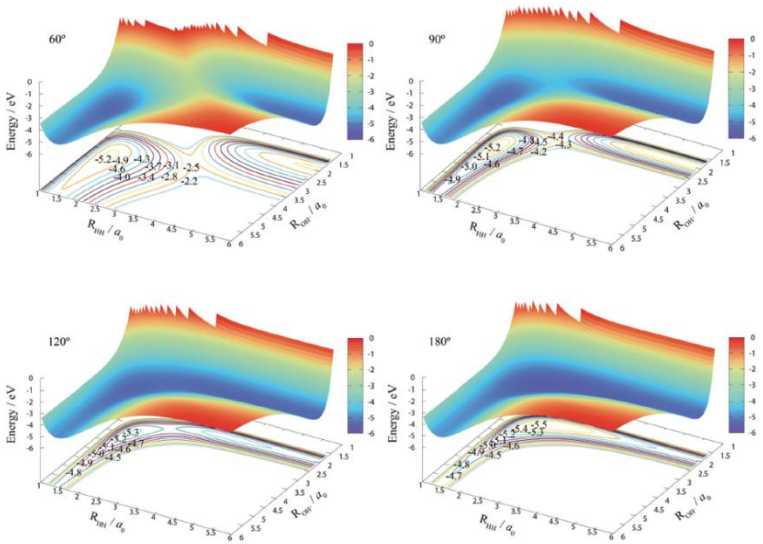

Fig. 2 Potential energy surfaces for O^+–H–H angles of 60°, 90°, 120°, and 180°.

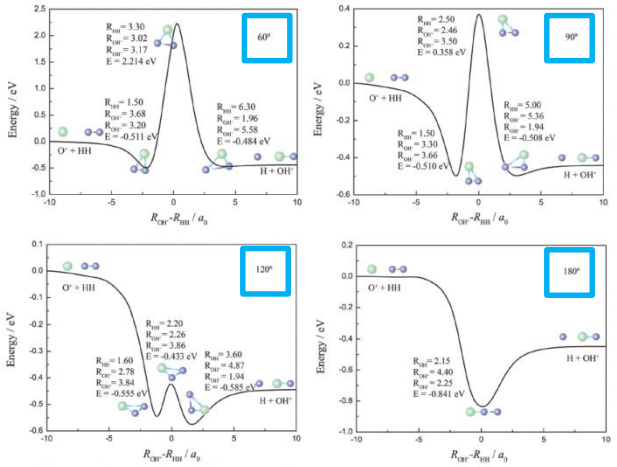

Fig. 3 Minimum energy paths for the new PES at four O^+–H–H angles.

Minimum energy paths

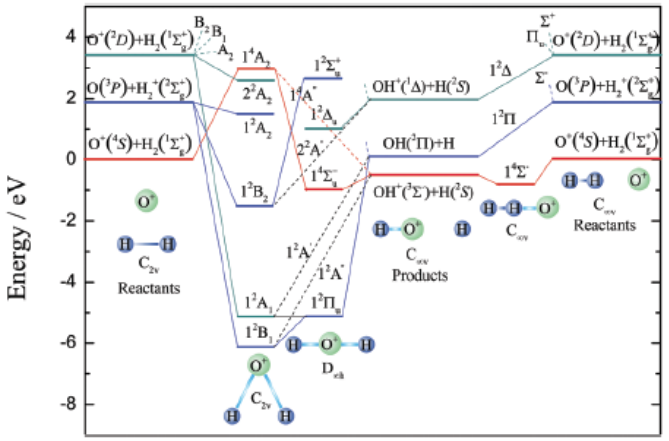

Fig. 1 Electronic correlation diagram for reactant, intermediate, and product arrangements of the H_2O^+ system under C_{2v}, $C_{\infty v}$, and $D_{\infty h}$ symmetries. The PESs of the title reaction are plotted by the red lines. This diagram is an adaptation of that reported in ref. 24.

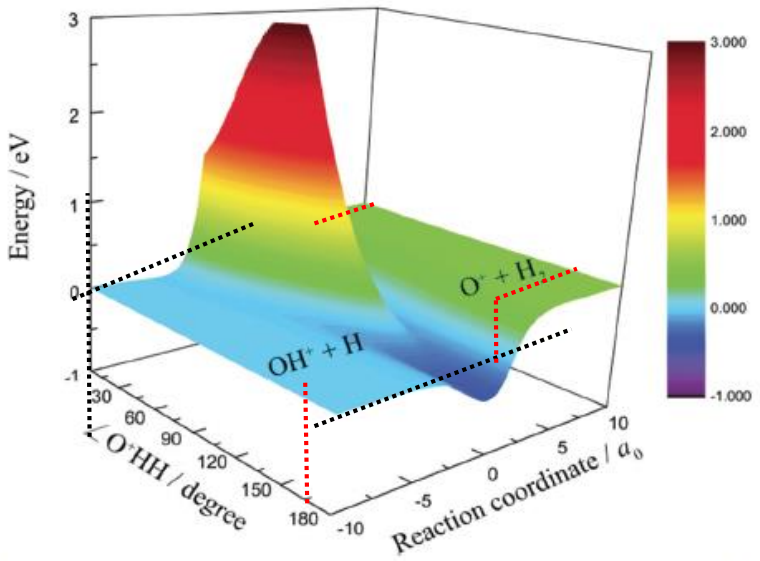

Fig. 4 Minimum energy paths of the new PES as a function of the bond–bond angle.

Reaction Coordinate

Reaction Coordinate

Henri Louis Le Chatelier
(1850-1936)

Karl Ferdinand Braun
(1850-1918)

Princip akce a reakce

Při ovlivňování rovnováhy se uplatňuje princip akce a reakce aplikovaný na chemické děje, známý pod názvem ***Le Chatelierův-Braunův princip***:

Porušení rovnováhy vnějším zásahem (akcí) vyvolá děj (reakci), který směřuje ke zrušení účinku vnějšího zásahu (akce).

Franck – Condon factor

$$P_{if} \sim \langle \psi_{initial}. \psi_{final} \rangle^2$$

proportional

Franck Condon principle

James Franck
1882-1964
1925 Nobel prize

Edward Condon
1902-1974

Franck-Condon principle

The probability (or amplitude) of a simultaneous electronic and vibrational transition to a new "vibronic" state depends on the overlap between the wavefunctions of the ground and excited states.

Or:
Electrons move much faster than nuclei. For an electronic excitation to occur, the nucleic configuration should be optimal (the same).

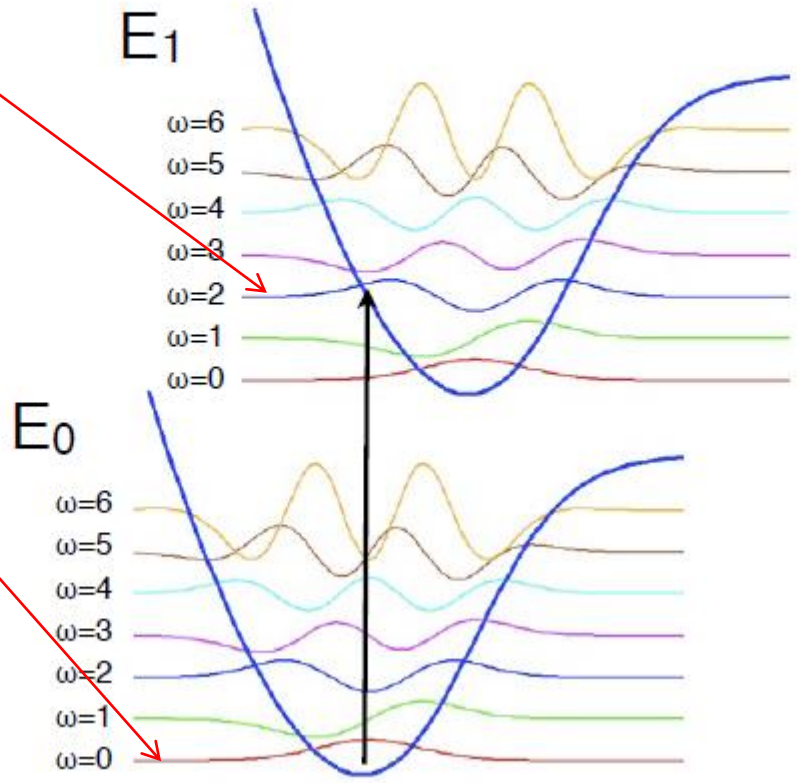

Transitions between molecular potential energy surfaces

During an electronic transition

the complex absorbs energy

electrons change orbital

the complex changes energy state

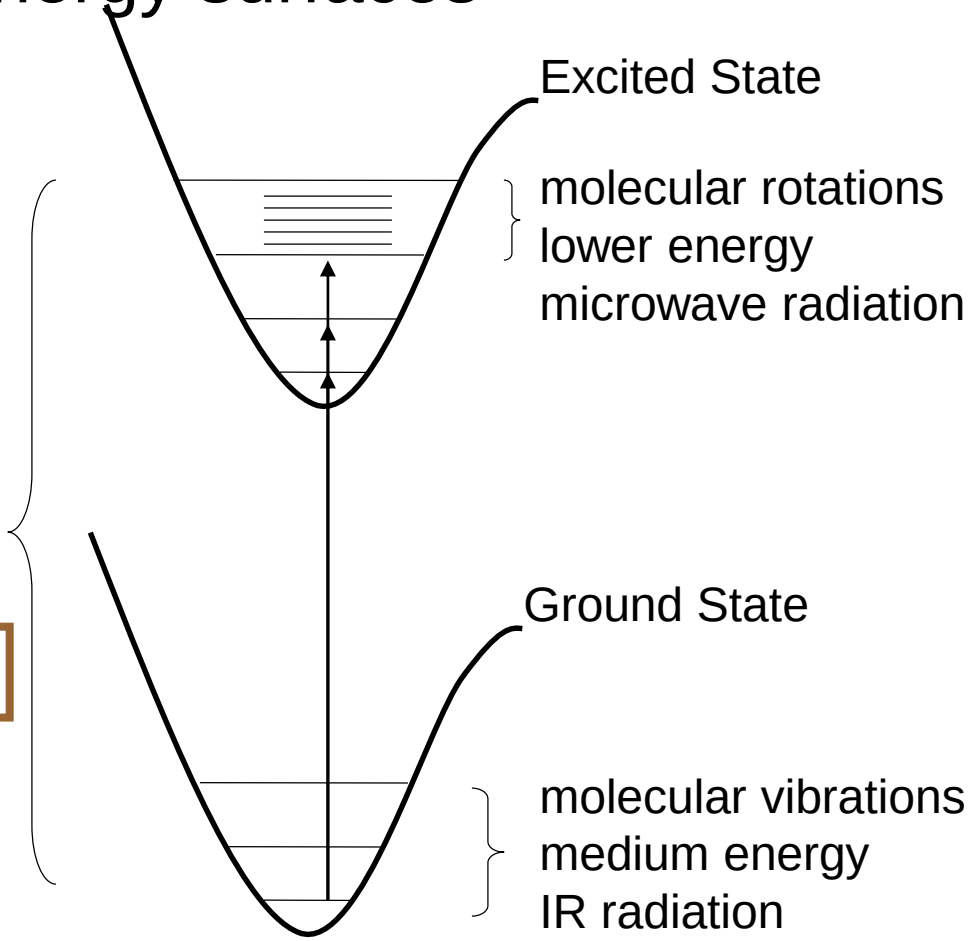

Electron: 1eV → $v=5.9\times10^{7}$ cm s^{-1}

$\tau \sim a_0/v \sim 10^{-8}/\ 5.9\times10^{7} = 2\times10^{-16}$ s

Timescale : ≈10^{-15} sec

Timescale of geometry changes (vibrations): ≈10^{-12} sec

As a result, observe vertical (Franck-Condon) transitions

In other words, we assume that we only have to consider the electronic portion of the ground- and excited-state wavefunctions to understand these transitions: Born-Oppenheimer approximation

The Born-Oppenheimer Approximation

The Born Oppenheimer Approximation assumes that electrons in a molecule move much faster than the nuclei, and adapt instantaneously, finding the lowest potential energy for each nuclear configuration. Therefore, it is possible to calculate an electronic energy for each nuclear configuration, considering the nuclei frozen.

Timescale : $\approx 10^{-15}$ sec

Timescale of geometry changes (vibrations): $\approx 10^{-12}$ sec

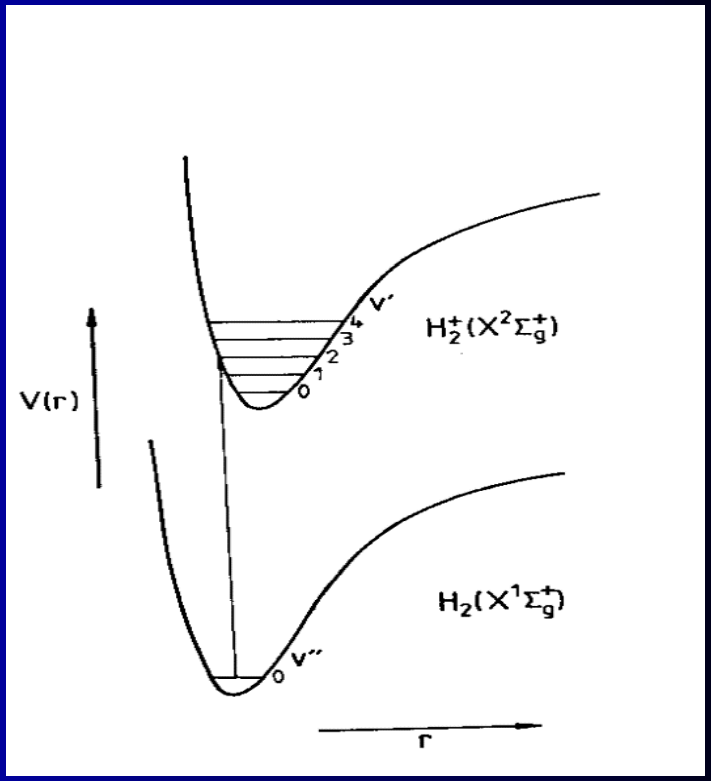

Condon approximation or *Franck-Condon principle*.

In the Condon approximation:

$$\int \Psi_F^* H_1 \Psi_I dx dQ = T_{fi}(Q=0) S_{v'v}$$

with $S_{v'v} = \int \tilde{\chi}_{v'}^*(Q)\chi_v(Q)dQ.$

$S_{v'v}$ and its square are *Franck-Condon overlap integral* and *Franck-Condon factor*, respectively (see also [2]).

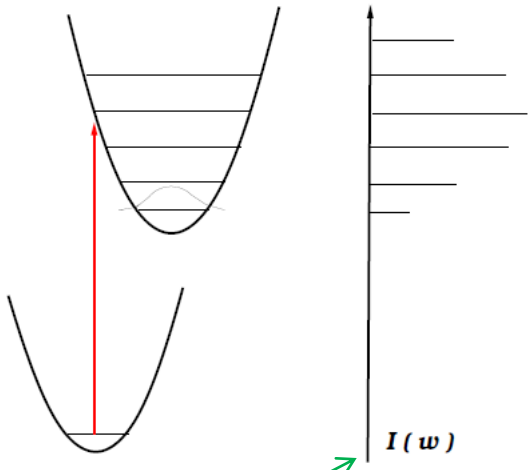

The spectrum follows immediately:

$$I(\omega_{ph}) \sim |T_{fi}(Q=0)|^2 \sum_{v'} |S_{v'v}|^2 \delta(\tilde{E}_{v'} - E_v - \hbar\omega_{ph})$$

The relative intensities are determined only through vibrational wave functions, electronic wave functions play almost no role.

Principle of vertical transitions !

$$P \sim \langle \psi_{initial}. \psi_{final} \rangle^{2.}$$

Franck – Condon factor

Absorption or emission of a photon

Collision with electron

The **Franck–Condon principle** is a rule in spectroscopy and quantum chemistry that explains the intensity of vibronic transitions. Vibronic transitions are the simultaneous changes in electronic and vibrational energy levels of a molecule due to the absorption or emission of a photon of the appropriate energy. The principle states that during an electronic transition, a change from one vibrational energy level to another will be more likely to happen if the two vibrational wave functions overlap more significantly.

The absorption or emission of a photon

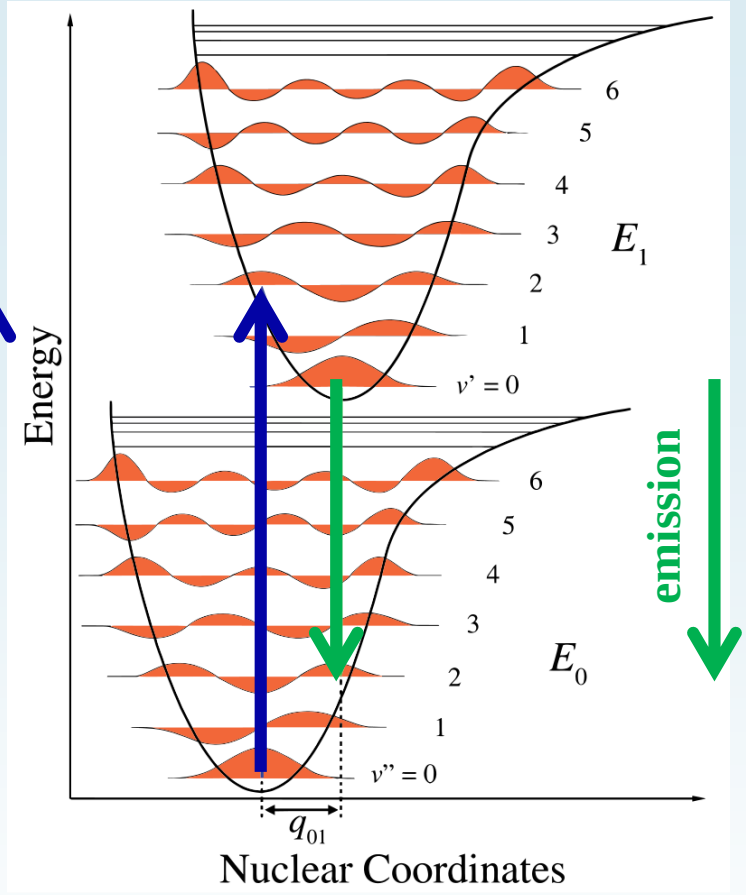

Franck–Condon principle energy diagram. Since electronic transitions are very fast compared with nuclear motions, vibrational levels are favoured when they correspond to a minimal change in the nuclear coordinates. The potential wells are shown favouring transitions between $v = 0$ and $v = 2$.

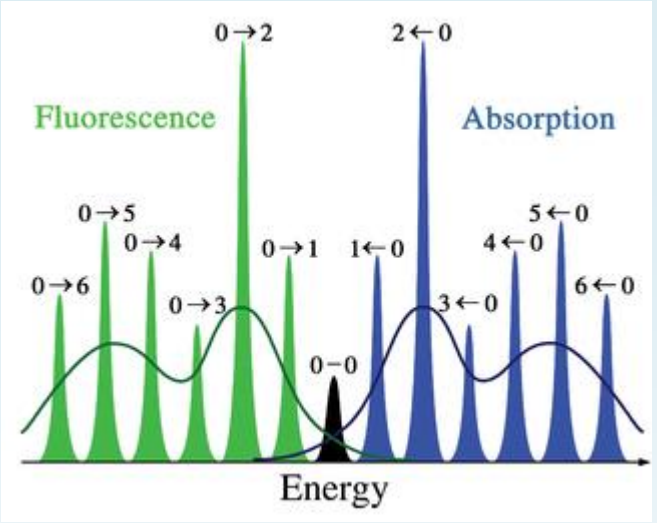

Schematic representation of the absorption and fluorescence spectra corresponding to the energy diagram in Figure 1. The symmetry is due to the equal shape of the ground and excited state potential wells. The narrow lines can usually only be observed in the spectra of dilute gases. The darker curves represent the inhomogeneous broadening of the same transitions as occurs in liquids and solids. Electronic transitions between the lowest vibrational levels of the electronic states (the 0–0 transition) have the same energy in both absorption and fluorescence

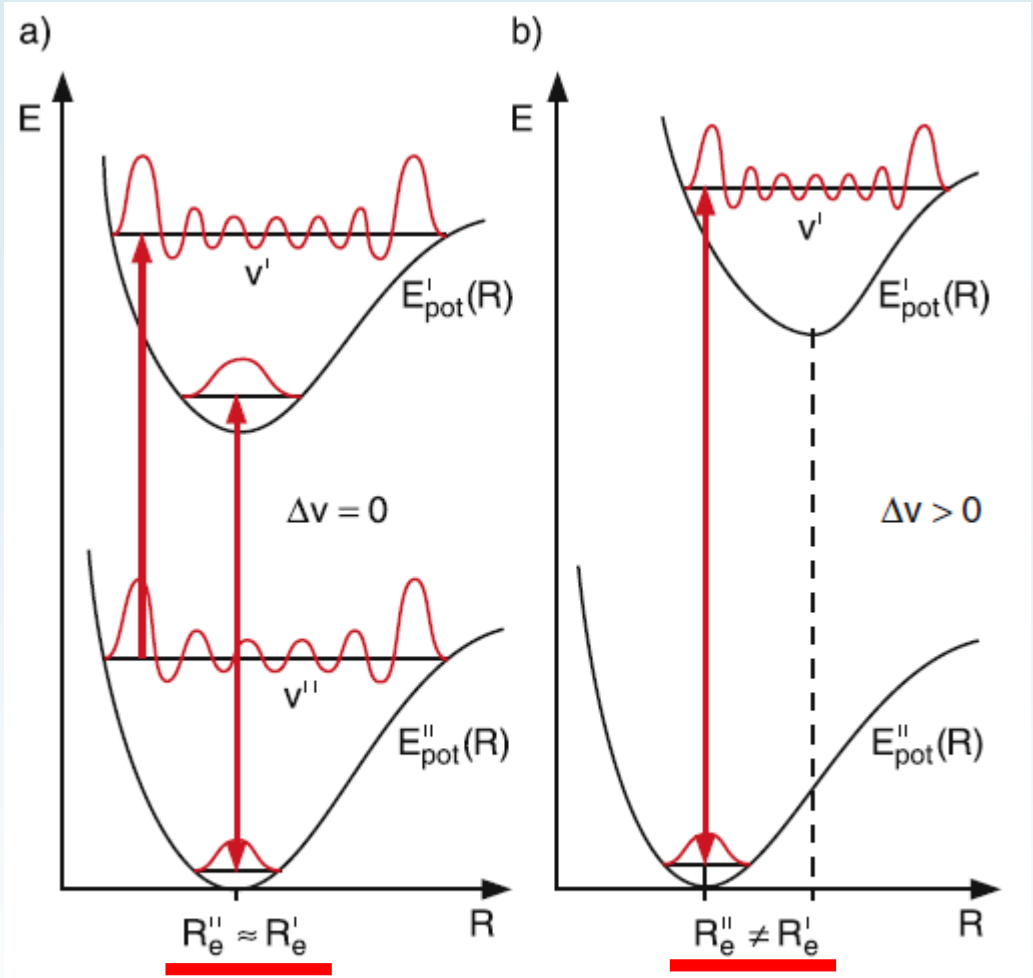

Fig. 9.62. Illustration of the Franck-Condon principle for vertical transitions with $\Delta v = 0$ (**a**) and $\Delta v > 0$ in case of potential curves with $R''_e = R'_e$ and $R'_e > R''_e$

Photoelectron spectrum H_2

$$P \sim \langle \psi_{initial}.\ \psi_{final} \rangle^{2}.$$

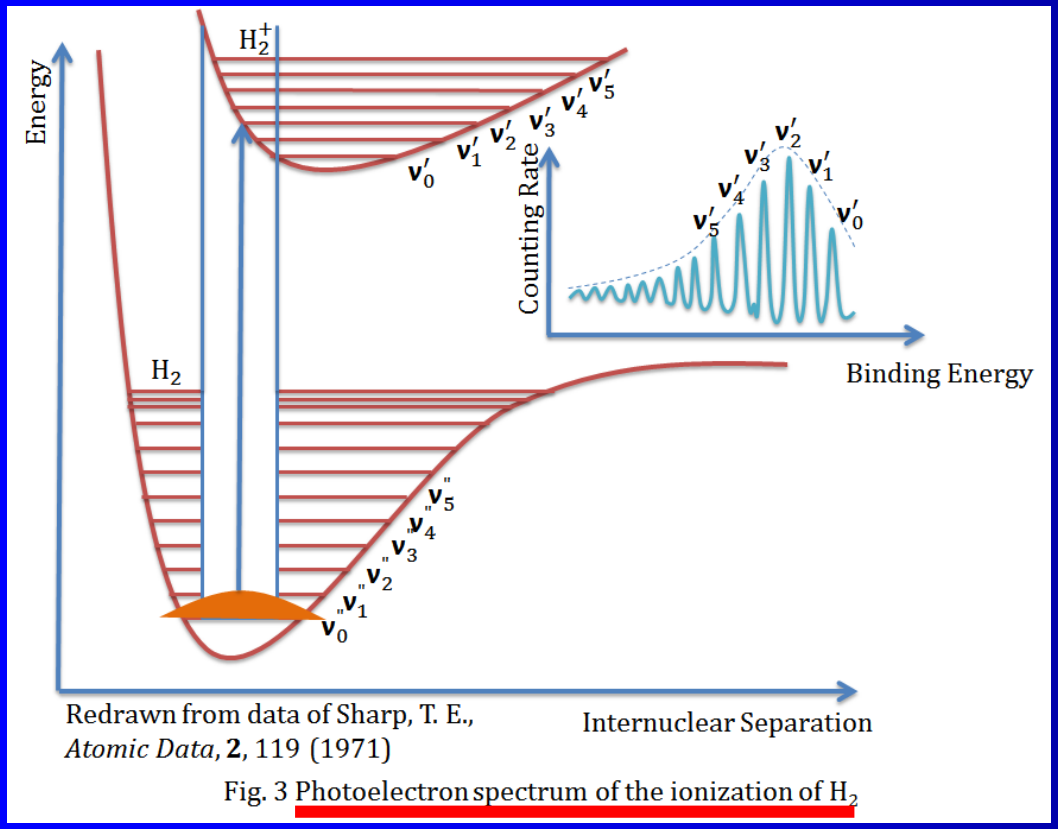

Fig. 3 Photoelectron spectrum of the ionization of H_2

Franck-Condon Principle

- Absorption of light and promotion of an electron from one state to another happens rapidly.
- Because of the short time it takes for the electronic transition, there is little or no geometry change in the molecular system.
- As a result, we say that **electronic transitions occur vertically** on a potential energy diagram.

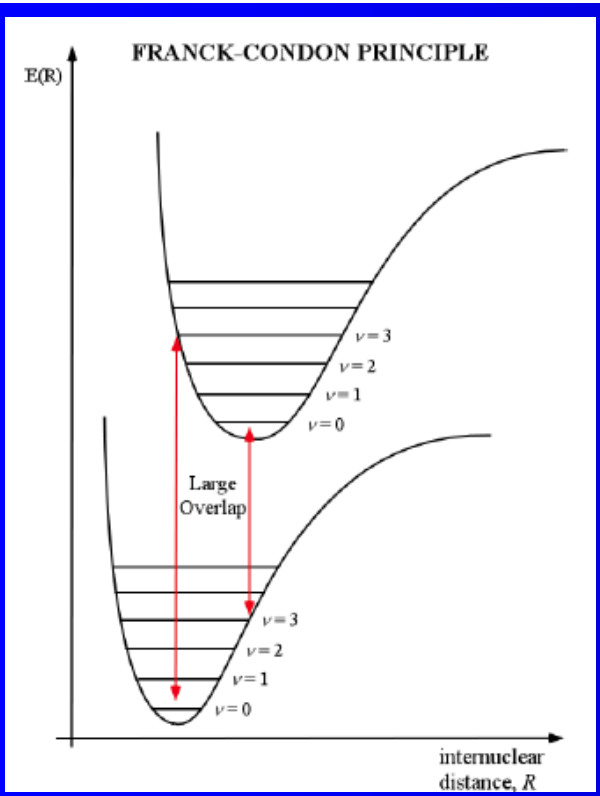

Franck-Condon Principle

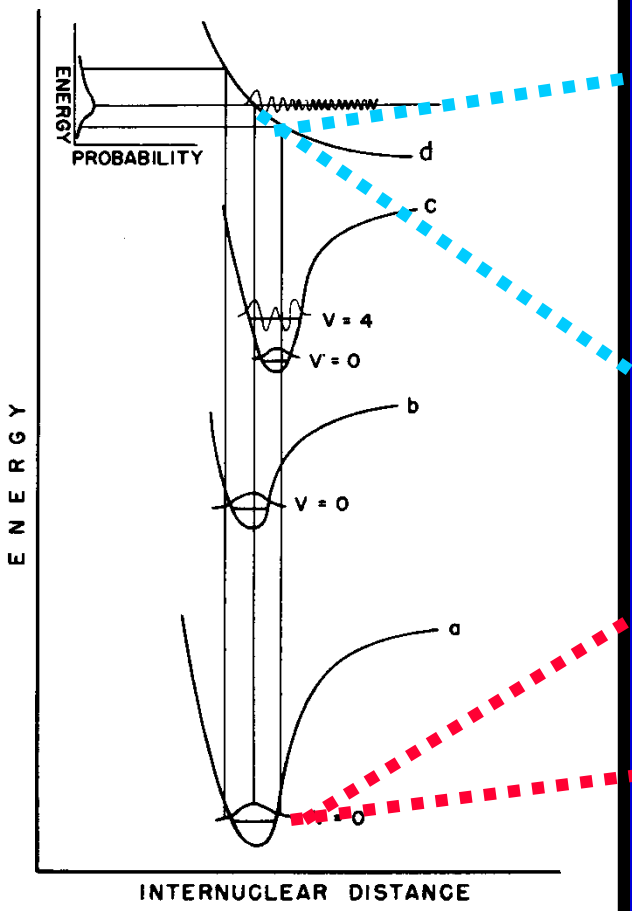

FIG. 21. Illustrative diatomic molecule and molecule-ion potential energy curves. The actual energy difference between curves a and b, c, and d is much greater than represented.

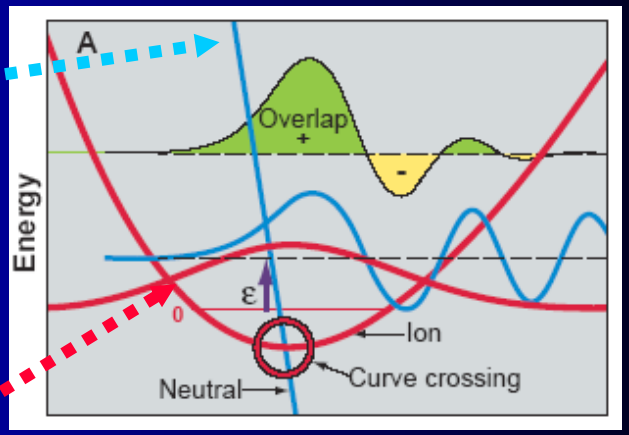

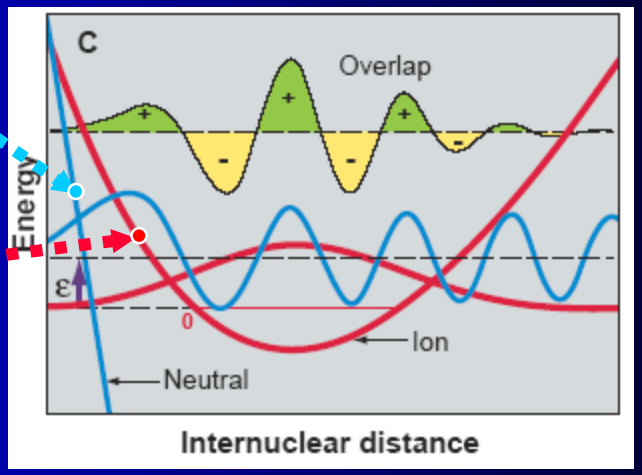

Franck-Condon Factors

$$P \sim \langle \psi_{initial}. \psi_{final} \rangle^{2.}$$

Franck-Condon principle - FOTOIONIZATION

MO diagram for the three highest occupied MOs in CO accessible by HeI radiation. PES of CO obtained by HeI radiation and potential energy curves for the neutral molecule and the three ionized states.

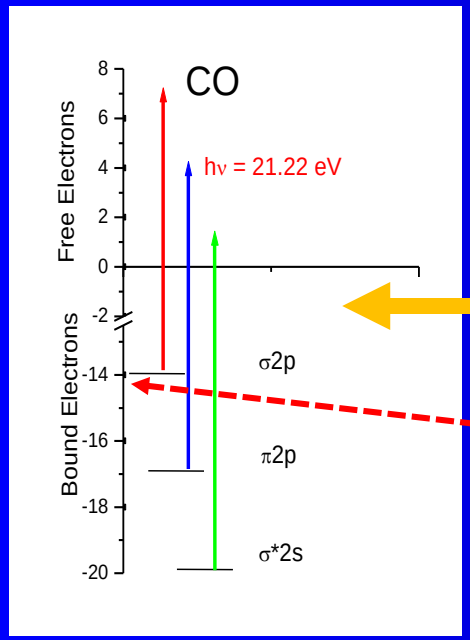

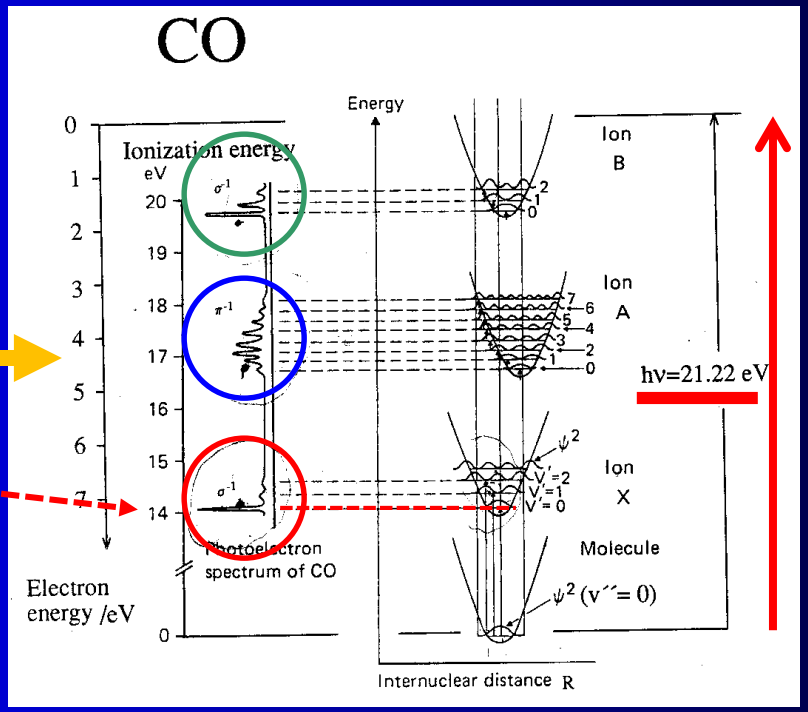

IE of CO ~ 14 eV

4.5.1 Dynamics of electronically excited states

- A molecule which is electronically excited by (laser) radiation can undergo a range of dynamical processes:

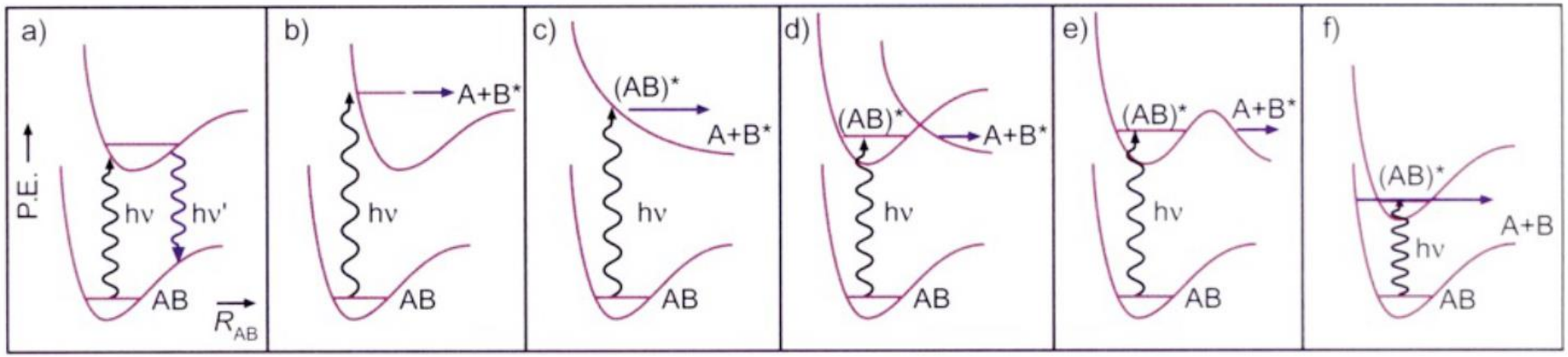

a) Laser-induced fluorescence
b) Excitation to the repulsive wall of a bound state, leading to direct dissociation
c) Excitation of a repulsive state, leading to direct dissociation
d) Excitation to a bound state and dissociation by coupling to a repulsive state
e) Excitation to a bound state and dissociation by tunneling through a barrier
f) Excitation to a bound state and dissociation by internal conversion to the dissociation continuum of the ground state

Processes d)-f) are referred to as predissociation.

Details of interaction of electron with molecules

Details of interaction of electron with H_2

Potential Energy Surface Description of the Ionization of Dihydrogen

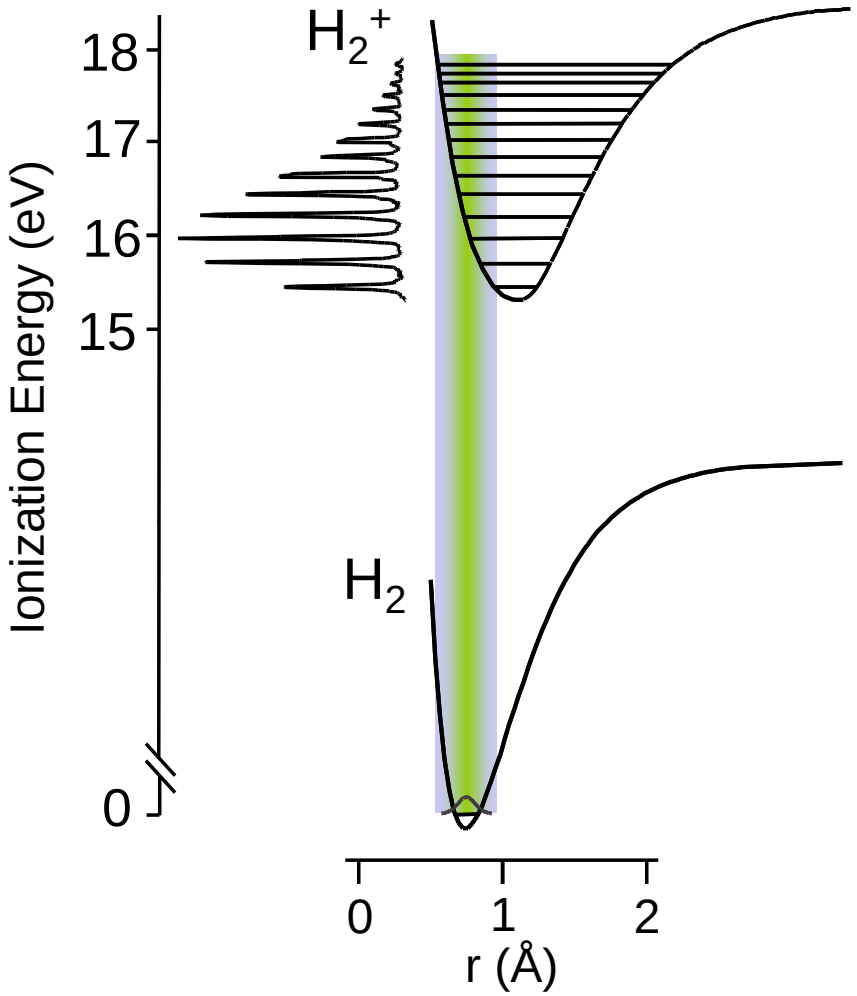

PES of H2

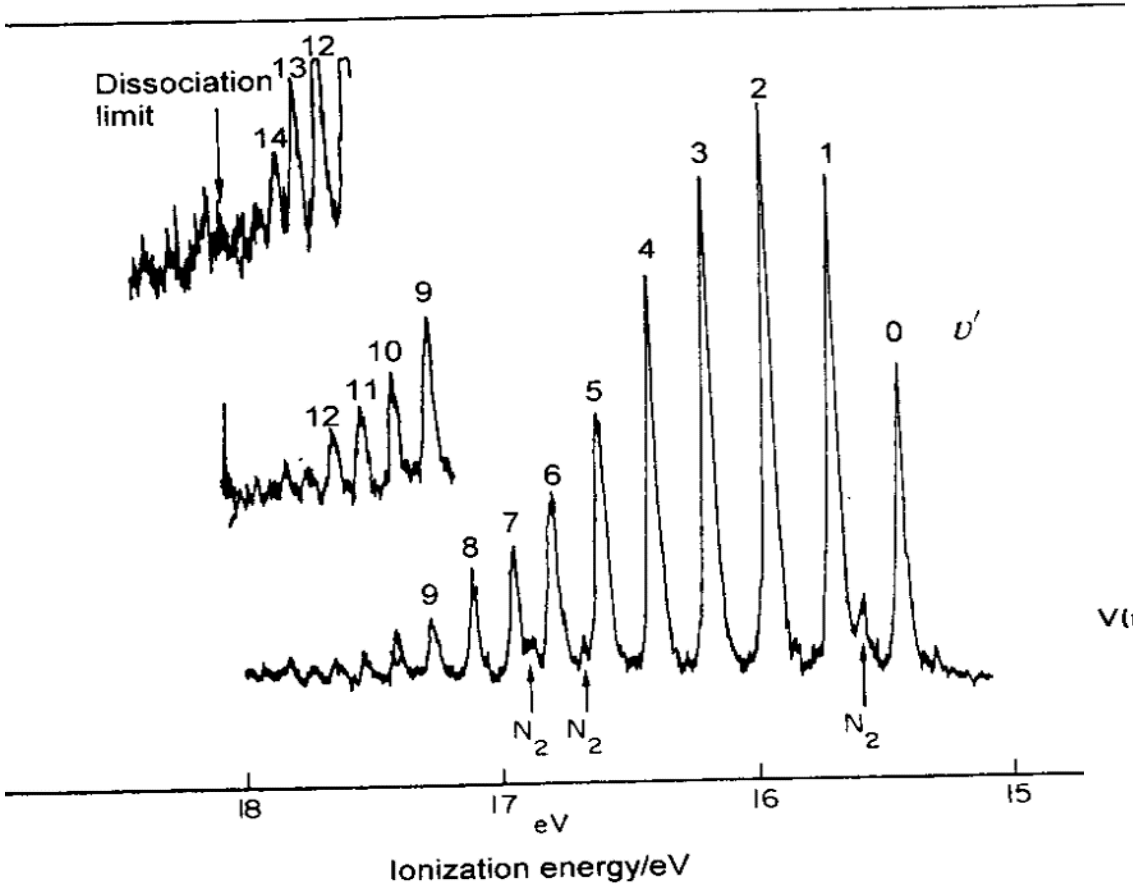
Dissociation limit
13
12
14
9
10
11
12
4
3
2
1
0
υ′
5
6
7
8
9
N2
N2
N2
18
17
eV
16
15
Ionization energy/eV

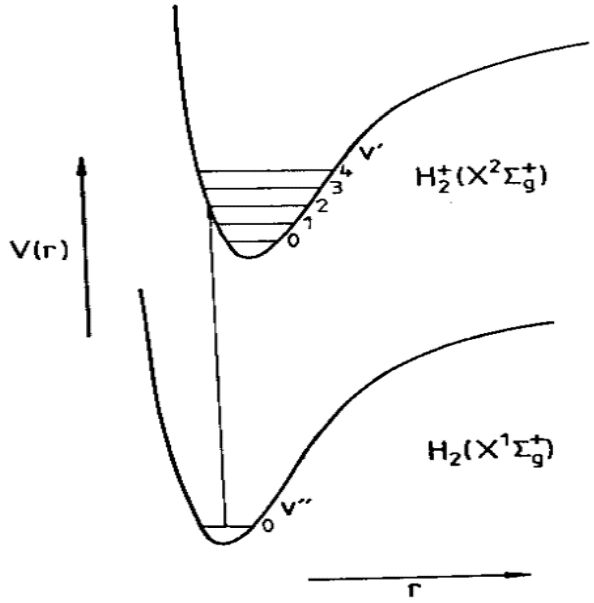
V(r)
v′
3
2
1
0
H2+(X2Σg+)
H2(X1Σg+)
v″
0
r

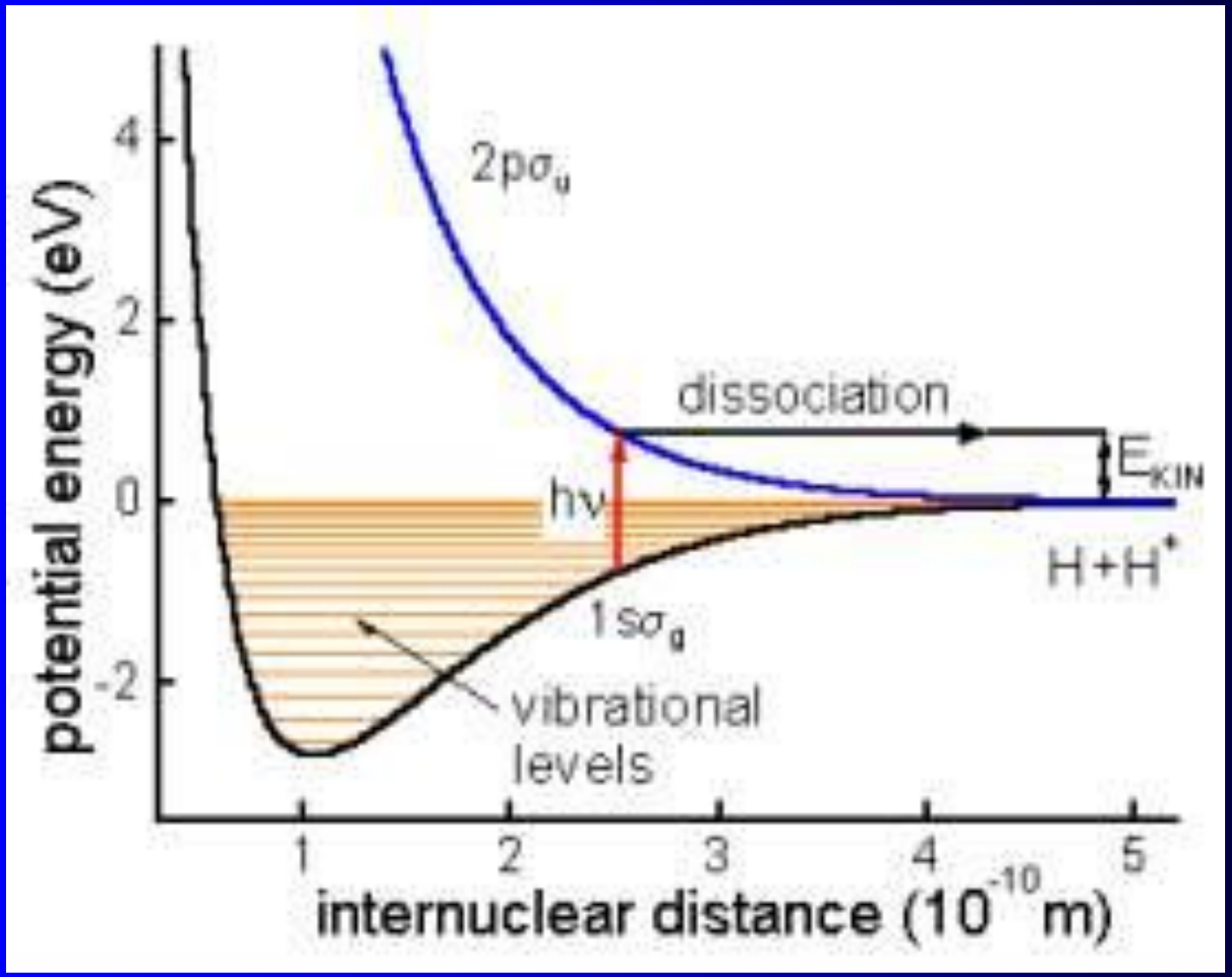
potential energy (eV)
4
2
0
-2
1
2
3
4
5
internuclear distance (10^{-10} m)
$2p\sigma_u$
dissociation
E_{KIN}
hν
$H+H^+$
$1s\sigma_g$
vibrational
levels